Chem Soc Rev

Post-synthetic Metalation of Metal-organic Frameworks

Journal:	*Chemical Society Reviews*
Manuscript ID:	CS-REV-02-2014-000076.R1
Article Type:	Review Article
Date Submitted by the Author:	31-Mar-2014
Complete List of Authors:	Evans, Jack; The University of Adelaide, School of Chemistry & Physics Sumby, Christopher; The University of Adelaide, School of Chemistry & Physics Doonan, Christian; The University of Adelaide, School of Chemistry & Physics

Post-synthetic Metalation of Metal-organic Frameworks

Jack D. Evans, Christopher J Sumby and Christian J. Doonan*

School of Chemistry and Physics, Centre for Advanced Nanomaterials, The University of Adelaide, Adelaide, South Australia, 5005.

Abstract

Post-synthetic metalation (PSMet) offers expansive scope for a targeted approach to tailoring the properties of MOFs. Numerous methods for carrying-out PSMet chemistry have been reported, however, these can be can be categorized into three general strategies: a) addition to coordinating groups; b) counter-ion exchange in charged frameworks; or, c) host-guest encapsulation of metal-containing entities within the pores of the framework. PSMet has been applied to enhance the performance characteristics of parent MOFs for gas storage and separation, and catalysis. Notably, PSMet is a prominent strategy in the field of MOF catalysis as it offers a route to design size-selective catalysts based on the premise of reticular chemistry in MOFs and the ability to incorporate a range of catalytically-active metals centres Other applications for materials produced via or utilising PSMet strategies include enhancing gas storage or molecular separations, the triggered release of drugs, sensing and tunable light emission for luminescent materials. This review surveys seminal examples of PSMet to highlight the broad scope of this technique for enhancing the performance characteristics of MOFs and to demonstrate how the PSMet concept can be developed for future applications.

1. Introduction

Metal-organic Frameworks (MOFs) are a class of porous materials that have seen rapid and extensive growth.[1] MOFs are of particular interest to chemists as they are constructed by a modular 'bottom-up' synthetic approach that enables precise spatial control of chemical moieties within the framework architecture. Furthermore, the vast number of organic links and inorganic nodes that can be combined give rise to prodigious scope for generating novel materials.[2] Access to such a variety of novel porous solids has prompted chemists to utilise MOF pore

networks as a host matrix for extraneous metals. The ultimate motivation for exploring such 'post-synthetic metalation' (PSMet) is to imbue the parent MOF with enhanced capabilities for applications, including gas adsorption and separation, sensing, and catalysis. Indeed, this review provides many examples of how PSMet strategies have been successfully employed to give access to materials for targeted practical applications. We note that PSMet is a subset of the more general post-synthetic modification (PSM) approach to functionalising MOFs. Thus, in this review we will use the abbreviation 'PSMet' in this to make this distinction clear.

Extraneous metals can be incorporated into the MOF pores via four main strategies as outlined in Scheme 1 and discussed in Section 2. These are: a) addition to functional groups that are either part of the organic link, appended to the organic backbone via post-synthetic methods, or anchored to the metal node of the framework; b) counter-ion exchange in charged frameworks; c) growth or encapsulation of metal nanoparticles or compounds within the pores of the framework; and, d) cation metathesis at the metal nodes. We note that this review will focus on post-synthetic strategies to introduce metals to a framework that are non-structural i.e. it will not include studies on cation metathesis at the metal nodes. We invite the reader to see the review by Dincă and co-workers in this current edition of Chem. Soc. Rev. for a thorough exposition on this topic.[3] A salient feature of PSMet is that the MOF remains isostructural throughout the synthetic process. Given that a non-metalated framework can be selected based on a particular set of structure metrics (e.g. pore shape and size) a strategic approach to designing novel functional materials is possible. A straightforward example would be the design of a size-selective catalyst by PSMet of a MOF with chosen pore dimensions. Of course certain considerations must be taken into account, such as the available free space that is assumed by the extraneous metal and its associated ligands or cations. Nevertheless, in principle, PSMet offers expansive scope for a targeted approach to tailorable materials for catalysis.

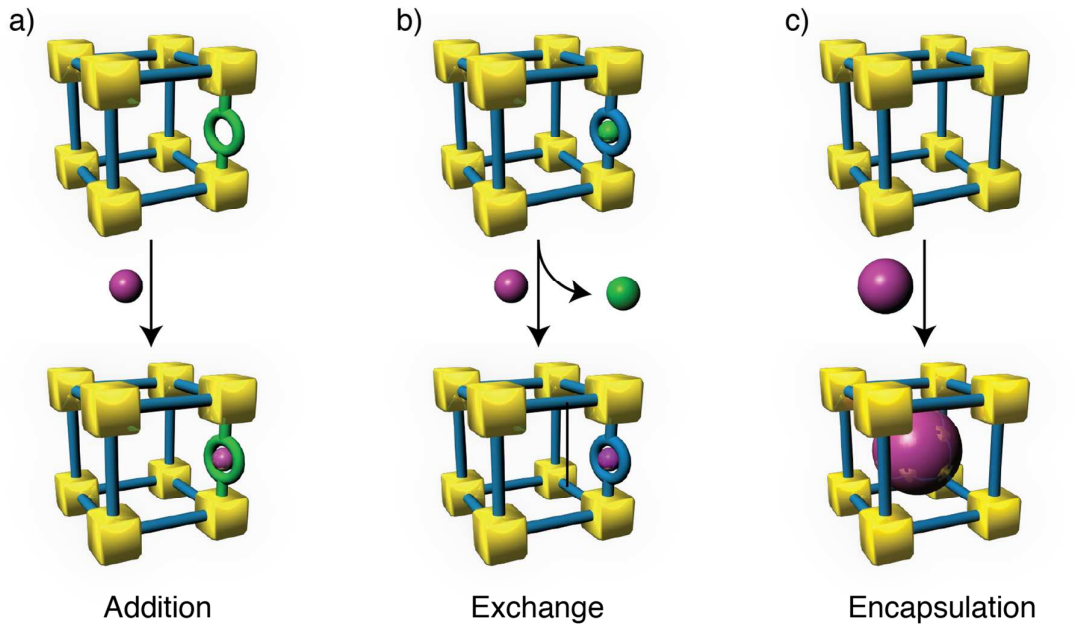

Scheme 1. Routes to post-synthetic metalation (PSMet) via (a) addition, (b) exchange and (c) encapsulation. One unit of the MOF structure is shown with the yellow cubes used to represent the metal node and blue rods the organic linkers. The organic components or the ions involved in PSMet are highlighted in green and the extraneous metal species depicted by a purple sphere. The number of organic links within a repeat unit of the MOF that undergo PSMet are system dependent on its structure; only one organic link is shown in the above examples for clarity.

MOFs have attracted interest as a platform for exploring PSMet chemistry largely due to their fundamental structural characteristics and design principles that yield significant control over the framework architecture and pore chemistry. For example, the structure metrics of a given MOF can be altered while retaining the underlying topology of the material. This concept which has been termed 'reticular chemistry'[4] offers the potential to fine tune the pore environment to facilitate PSMet. Another aspect of MOFs that renders them poised for PSMet studies is the chemical mutability of the core building components. A wide range of metal binding groups can be incorporated into the ligand structure or be post-synthetically constructed in the pores of the MOF. In addition, there are several examples where the metal node has been used as a site for anchoring functional groups to the MOF. The availability of both the organic and inorganic building units for PSMet manifests in the versatility of MOFs to support diverse PSMet

chemistry. Finally, the structural robustness and high degree of long range order are general characteristics of MOFs that underpin the capacity to carry-out post-synthetic chemistry and afford well characterised materials. An advantage of high crystallinity, compared to amorphous solids, is that the position of each atom is precisely known in 3D space. Accordingly, metal ions can be post-synthetically incorporated into the framework at predetermined positions throughout the material, with clear factors favouring positioning in proximity to the metal nodes or the linkers depending on the targeted applications. Such well-defined and located moieties are of significant interest to chemists as they are crucial to the judicious design of functional materials applicable to catalysis, gas storage, separations, metal sensing and sequestration, light emitting materials and drug delivery.[5] Discussion of how PSMet approaches facilitate such applications is described in section 3. A further requirement of the PSMet strategy is that the parent material retains its structural properties after sequential chemical reactions. MOFs are known for high thermal stability and work has moved towards developing systems that are also structurally resistant to aqueous media[6] and what would be considered harsh reaction conditions, i.e. concentrated acid and base.[7] These examples have engendered novel developments in PSMet chemistry, leading to applications in the areas noted above.

This review aims to introduce the reader to the general strategies that have been employed to perform PSMet on MOFs. Rather than provide an exhaustive survey of the literature we endeavour to cite seminal examples of PSMet that highlight particular general features of the approach, and will evince the exciting and broad scope of this technique. In addition, by way of further selected examples, we will illustrate how PSMet has been applied to enhance the performance characteristics of parent MOFs and canvass the potential for future applications in heterogeneous catalysis, gas storage and molecular separations, metal sensing sequestration of toxic metals, for tuneable light emission and drug delivery.

2. Synthetic Approaches towards PSMet

2.1 Metal Addition

Post-synthetic metal addition to frameworks has been a widely exploited reaction manifold which utilises, at some stage, reactive functional groups introduced during or after MOF synthesis. Six main strategies have been explored (Scheme 2), including addition to non-coordinated metal binding groups, orthogonal deprotection of a metal binding moiety and PSMet, post-synthetic construction of a binding site followed by PSMet, outright linker exchange, or direct framework addition by the formation of a new organometallic entity. The ensuing section, which highlights salient examples of PSMet addition, examines their individual pros and cons.

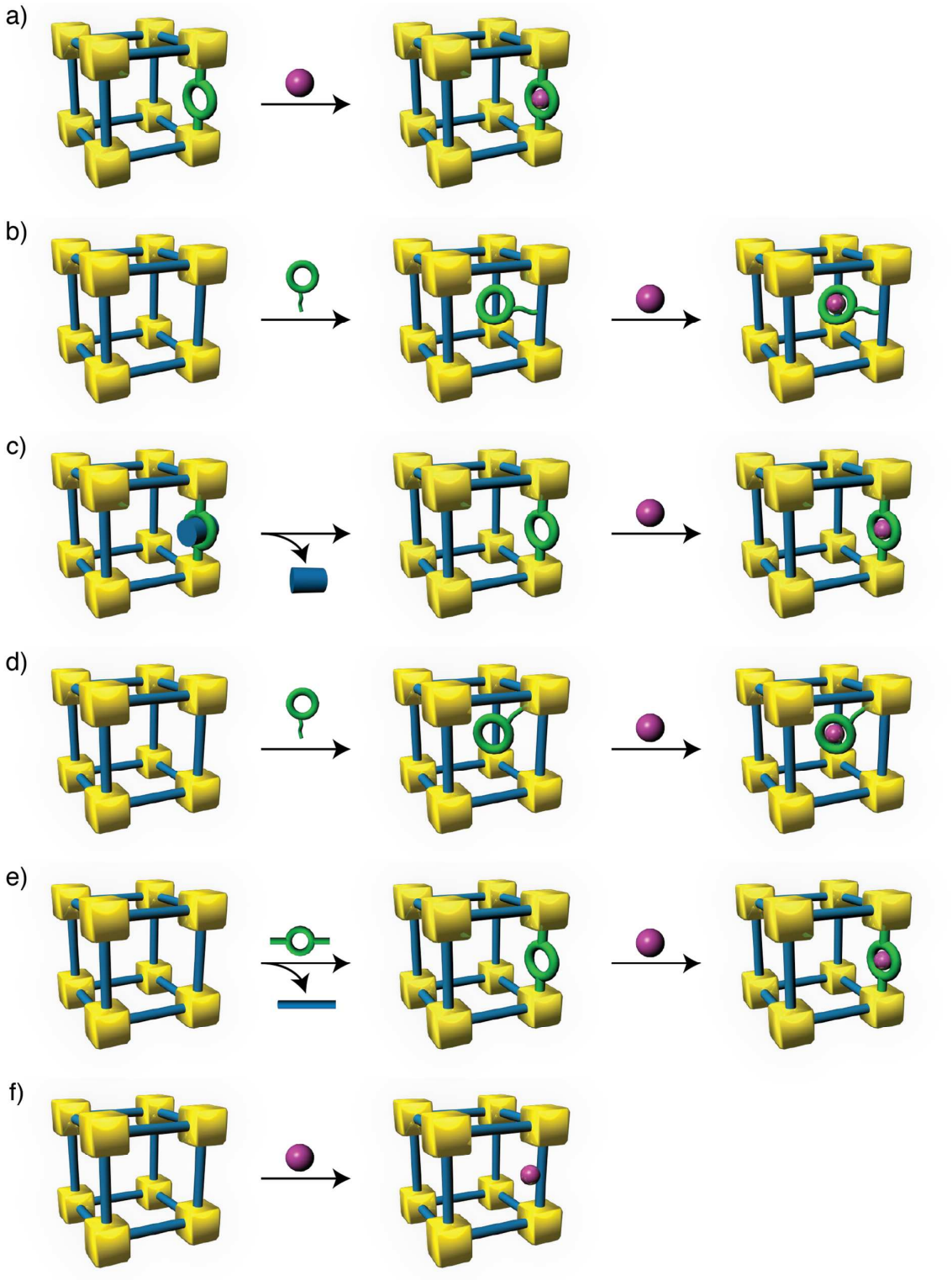

Scheme 2. Routes for PSMet addition to MOFs. (a) PSMet of non-coordinated metal binding groups. PSMet by (b) construction of a binding site at the linker, (c) liberating binding groups by an orthogonal deprotection step or (d) formation of a coordinating site at a node. Further addition strategies include (e) outright linker exchange, or (f) direct framework addition during the formation of a new organometallic entity. In (a)–(f) the purple sphere represents the post synthetically added metal, the green toroids represent metal-binding moieties

and the blue cylinder represents a metal that is introduced into the framework backbone before or during MOF synthesis as a protecting group.

2.1.1 Addition to non-coordinated metal binding groups.

A successful PSMet strategy for incorporating metals into MOF pore cavities has been to imbue the organic backbone with donor sites capable chelating a metal centre that is non-structural in the context of the MOF (Scheme 2a). This approach can be carried-out by employing ligands that have both primary and secondary functional groups.[8] In this case the primary functional group denotes the structure-forming component of the ligand, generally pyridyl or carboxylate donors, and the secondary functional group is designed to bind the extraneous metal ion. The effectiveness of this approach relies upon the secondary functional group being compatible with the framework synthesis, i.e. that it does not hinder MOF formation or become a structural motif, thus rendering it incapable of binding to post-synthetically added metals. Furthermore, strategies that allow PSMet to occur at a free chelating site within a MOF has engendered metalated MOF materials with greater chemical stability, due to the chelate effect, for ensuing applications.

A seminal example of this technique was reported by Lin and co-workers[8] who employed, chiral, (*R*)-6,6-dichloro-2,2-dihydroxy-1,1'-binaphthyl-4,4'-bipyridine (**1**, Figure 1), as the organic building block for a homochiral cadmium-based MOF. The synthesis of this MOF possessing free secondary dihydroxy functional groups without use of protecting groups was accomplished by judicious use of a soft Lewis acid as the metal node, which binds in preference to the borderline hard/soft Lewis basic pyridyl donors rather than the hard ROH/RO- chelating site. In this example the secondary dihydroxy functional groups were post-synthetically metalated with $Ti(O^iPr)_4$ thus lining the pores of the MOF with a catalytically active Lewis acid moiety. However, for this system the metal occupancy of the dihydroxy ligands or a demonstration of permanent porosity of the metalated framework was not canvassed.

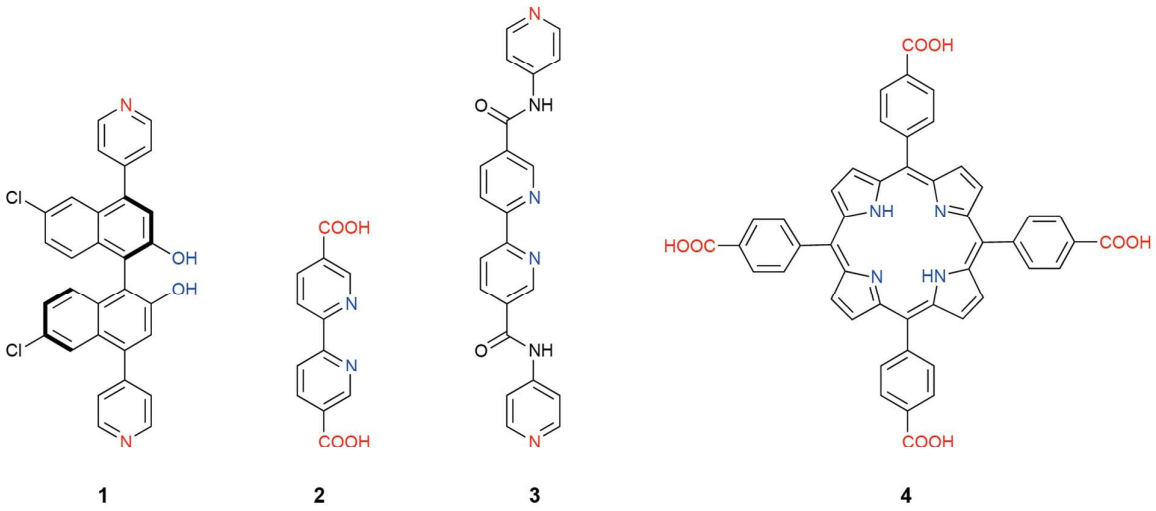

Figure 1. Chemical structure of linkers **1**-**4** with primary (red) and secondary (blue) functional groups.

Subsequently, in the reversal of the strategy employed above, Bloch *et al.* reported the first example of a MOF containing free 2,2'-bipyridine (bipy) building units with borderline hard/soft Lewis basic donors.[9] The propensity of bipy ligands to strongly bind a wide variety of transition metals potentially limits the compatibility of these types of ligand for MOF synthesis. Accordingly, oxophilic Al^{3+} ions were utilised in order to coordinate the relatively hard Lewis basic carboxylates in preference to the softer nitrogen donors. Indeed reaction of 2,2'-bipyridine-5,5'-dicarboxylic (bpydc, **2**) acid with $AlCl_3{\cdot}6H_2O$ yielded a novel MOF (MOF-253) with bipyridine donors poised for PSMet studies. ^{27}Al MAS NMR of the bulk activated solid showed a single peak attributed to the six-coordinate Al^{3+} site of the metal node, thus verifying that the bipy donors remained unoccupied. PSMet of the bipy sites with $Cu(BF_4)_2$ and $[PdCl_2(CH_3CN)_2]$ yielded high metal occupancy ($Al(OH)(bpydc){\cdot}0.83PdCl_2$ and $Al(OH)(bpydc){\cdot}0.97Cu(BF_4)_2$) according to elemental analysis. These values are consistent with the strong metal binding capacity of the bipy unit. In addition, Extended X-ray Adsorption Fine structure (EXAFS) experiments were used to confirm that the N_2PdCl_2 unit was of an analogous structure to the molecular species $(bipy)PdCl_2$, highlighting the importance of this technique in accurately identifying the nature of the metalated species. An important aspect of this work is that permanent porosity and structural order were preserved subsequent to PSMet experiments, although the surface areas and pore volumes are reduced commensurate with increasing the occupancy of the metal sites of the

framework; i.e. for 1·0.08$PdCl_2$ and 1·0.83$PdCl_2$ N_2 adsorption measurements at 77 K resulted in type I adsorption isotherms with reduced BET surface areas of 1780 and 355 m^2/g, respectively (versus 2160 m^2/g for MOF-253) and estimated pore volumes for the samples were lowered to 0.65 and 0.13. Furthermore, the authors clearly showed that secondary functional groups with a high metal affinity, such as bipy, could be part of the ligand used to construct MOFs. Both the strategies introduced above indicate that MOFs possessing free secondary metal binding functional groups can be prepared via one-pot syntheses upon judicious choice of metal ions and reaction conditions, with due consideration of the Lewis acid/base properties of the metals and donor groups involved. Utilising the same strategy and MOF, Martín-Matute *et al*. report the formation of [Ru(bpy)Cl_3(dmso)] entities within the MOF by PSMet.[10] Here the 13% metalated product (Al(OH)(bpydc)·0.13$RuCl_3$(DMSO) had very low BET surface areas but a 7% metalated product (Al(OH)(bpydc)·0.7$RuCl_3$(DMSO) retained permanent porosity and was used to catalyse oxidation reactions of alcohols. This work demonstrates that both the nature of the post-synthetically added metal species and the PSMet conditions play a significant role in the properties of the final products.

Hardie and co-workers also synthesized an open framework with a coordinatively unsaturated bipy moiety using a mixed-link approach.[11] Reaction of Zn^{2+}, *N,N'*-bis(pyridin-4-yl)-2,2'bipyridine-5,5'-dicarboxamide (**3**) and isophthalic acid in a 1:1:1 ratio led to the formation of an extended network with metal free bipy moieties. PSMet with Cu^{II} resulted in a framework where two proximal bipy units are linked via a coordinated Cu^{I} ion. This example identifies that a mixed-link approach, which potentially reduces the number of metal binding sites, may be used to access metal free coordinating sites in an open framework, however, it is not yet clear if such a strategy could be generally applicable. If harnessed correctly, such a strategy could be used fruitfully to yield MOFs of similar structure metrics but with the capacity to control the metal loading and loss of available pore space.

Using an analogous strategy to Bloch *et al.*, permanently porous MOFs composed of metal free porphyrins have been recently synthesized by using oxophilic Zr^{4+} ions designed to preferentially bind the hard carboxylate donors of tetracarboxyphenylporphyrin linkers (**4**).[12, 13] These porphyrin MOFs are robust

and can exhibit surface areas in excess of 2000 m^2g^{-1} thus providing an excellent platform for PSMet studies. Indeed, Morris *et al.*[13] demonstrated that Fe^{3+} and Cu^{2+} could be incorporated into the metal free porphyrin networks. It is noteworthy that PSMet could effect quantitative incorporation of Fe^{3+}, however, the analogous MOF could not be formed using the pre-metalated porphyrin building block, indicating the importance of this technique as a route to novel materials.

Organic units that possess secondary functional groups with less well-defined binding modes have also been used to construct MOFs via one-pot syntheses. Due to the absence of the chelate effect the potential of these secondary functional groups to interfere with framework synthesis or occlude metal ions intended for structural nodes is minimised. As a consequence, the pores of such MOFs will be available to facilitate non-specific or generally less well defined binding of the post-synthetically added metal ions. Examples of monodentate secondary functional groups in MOFs where PSMet has been demonstrated include thioethers,[14, 15] hydroxides,[16, 17] aminopyridinato,[18] allyl,[19] thiols[20] and phosphines.[21, 22] Typically, the coordination motifs of the extraneous metals in these materials are characterised in the same manner as MOFs with defined coordinating groups, although the nature of metal binding can be a little more difficult to elucidate. Furthermore, such materials generally lack the stabilisation brought about the chelate effect and may be more prone to leaching of the PSMet added metal.

2.1.2 Addition to post-synthetically generated secondary binding sites

Another strategy for introducing structurally well-defined metal centres into the MOF pore network is to generate the metal binding moiety post-synthesis of the parent MOF. An obvious advantage of this approach is that framework synthesis can be executed without potential hindrance from the secondary functional group. However, this procedure requires, at minimum, a further synthetic step, which can compromise the structural integrity of the MOF. Three main strategies for realising a metal-free binding moiety in the MOF post framework synthesis are: 1) Post-synthesis ligand construction at the link (Scheme 2b), 2) Orthogonal deprotection of secondary functional groups (Scheme 2c), and 3) Grafting metal binding units on to the metal node (Scheme 2d).

Dynamic covalent chemistry has been the most widely employed strategy for constructing metal chelating groups within the framework pores. Specifically, imine chemistry shows great utility as it can be carried out under mild conditions and amino functionalities can be generally incorporated into the organic link without disrupting MOF formation.[23] An early example of this approach was demonstrated by Ingleson *et al*. who generated a salicylidene moiety in a MOF by performing a condensation reaction with salicylaldehyde and IRMOF-3 (Figure 2a).[24] We note that performing such precise solution chemistry on the molecular backbone of the MOF exemplifies the notion of 'crystals as molecules'.[25] The nascent salicylidene moiety was treated with $VO(acac)_2$ (acac = acetylacetonate) to afford a vanadyl complex with retention of bulk crystallinity as confirmed by PXRD experiments. A sub-stoichiometric conversion of the amine groups (13% conversion) was reported, which may be accounted for by steric encumbrance resulting from addition of the relatively large ligating group with respect to the pore cavity size (~7 Å). This observation emphasises that the structure of the host framework determines subsequent PSMet chemistry.

In light of this work, Yaghi and co-workers demonstrated that judicious selection of MOF topology can enhance the conversion to the metalated MOF and facilitate retention of structural order and permanent porosity following PSM.[26] In this work, 2-pyridinecarboxaldehyde was diffused into an amino functionalized MOF $(Zn_4O)_3(BDC\text{-}NH_2)_3(BTB)_4$, $H_2BDC\text{-}NH_2$ = 2-aminobenzene-1,4-dicarboxylic acid, H_3BTB = 1,3,5-tris(4-carboxyphenyl)benzene) to afford a structure replete with pyridylimine ligating groups. Subsequent reaction with $[PdCl_2(CH_3CN)_2]$ yielded $(Zn_4O)_3(BDC\text{-}C_6H_5N_2PdCl_2)_3(BTB)_4$ in quantitative yield. Saturation of the chelating ligand in this case was purported to arise from the large pore channels of the host MOF, which facilitate molecular diffusion and alleviate steric interactions between the post-synthetically introduced metal species. Furthermore, the structure of $(Zn_4O)_3(BDC\text{-}C_6H_5N_2PdCl_2)_3(BTB)_4$ is composed of two organic units and only one is functionalised with an amino group. This reduced metal:link ratio, with respect to a single component MOF, will also minimise potential steric crowding and may also contribute to the high PSMet yields observed.

The same parent multi-link framework was employed for PSMet studies (Figure 2b) by Tanabe *et al.*[27] However, in this case they showed that the amine group could undergo condensation reactions with functionalized anhydrides to generate multidentate metal binding sites within the MOF. The resultant frameworks were post-synthetically metalated with Cu^{2+} and Fe^{3+} and remained permanently porous throughout this process. Free carboxylate groups, designed for PSMet chemistry have also been introduced into MOF cavities via a post-synthetic reaction. This was achieved by diffusing succinic anhydride into a framework replete with naked hydroxyl functional groups.[28] The resultant ring-opening reaction engendered free carboxylic acid groups that were subsequently metalated with Cu^{2+} ions.

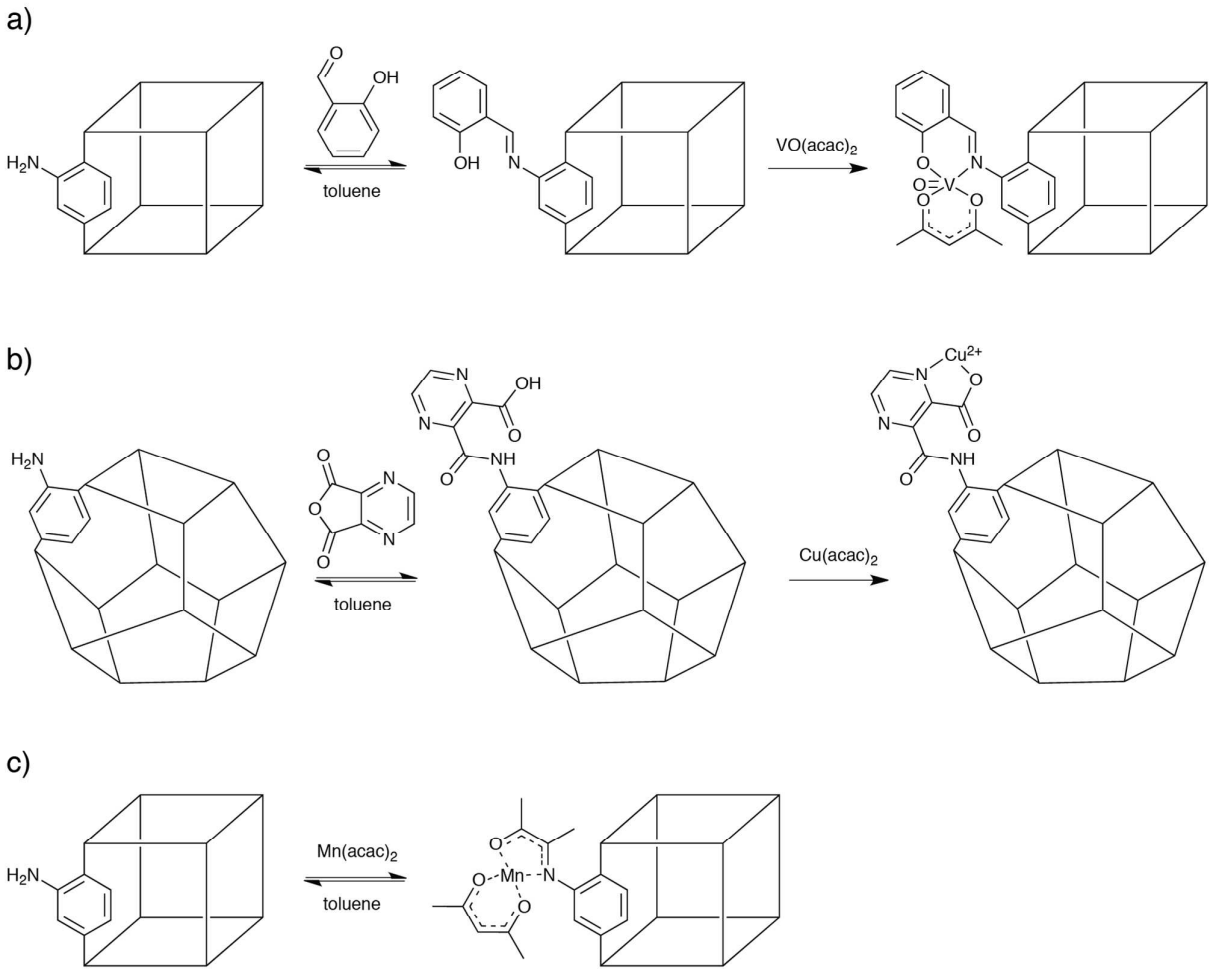

Figure 2. Examples of addition to post-synthetically generated secondary binding sites and direct, one-step attachment of metal complexes. (a) Schiff base formation within the pores of IRMOF-3 and treatment with $VO(acac)_2$ to afford a vanadyl complex. (b) PSMet studies on $(Zn_4O)_3(BDC\text{-}NH_2)_3(BTB)_4$ showing that an amine group could undergo condensation reactions with functionalized anhydrides. (c) An example of covalent addition of a pre-metalated ligand moiety

to IRMOF-3.[30] Schematic representations of one unit of the MOF structure are shown as polyhedra.

Rather than constructing metal binding groups via successive post synthetic modifications recent work has shown that such moieties can be grafted onto the organic backbone of MOFs in a pre-metalated form.[29-31] Under relatively benign conditions of toluene at 55°C, IRMOF-3 was treated with $Mn(acac)_2$ to yield a metalated MOF (Figure 2c).[30] Due to the benign conditions for PSMet the metalated MOF retained crystallinity and porosity (accounting for the addition of the metal complex). This methodology has great promise as it effectively reduces the number of post-synthetic steps required to introduce an extraneous metal into the pore framework. Accordingly, the potential for degradation of the MOF structure is reduced.

Another two step strategy (PSM followed by PSMet) for realising post-synthetic metal binding in MOFs without obstructing framework synthesis is to protect the secondary functional groups. These approaches draw upon an extensive repertoire of protecting group strategies available to the synthetic organic chemist and consequently show broad applicability for PSMet approaches. An important consideration here is that the protecting group should not alter the outcome of the MOF synthesis, and the deprotection step should be efficient and have minimal impact on the framework structure. With this in mind Tanabe *et al.*[32] showed that photochemical unmasking of catechol and hydroxy based functional groups was an effective approach (Figure 3). For example, they demonstrated that access to a catechol moiety could be achieved by the light driven cleavage of *o*-nitrobenzyl protecting groups. The free catechol group was used to bind Fe^{3+}, which was confirmed by UV-visible spectroscopy.

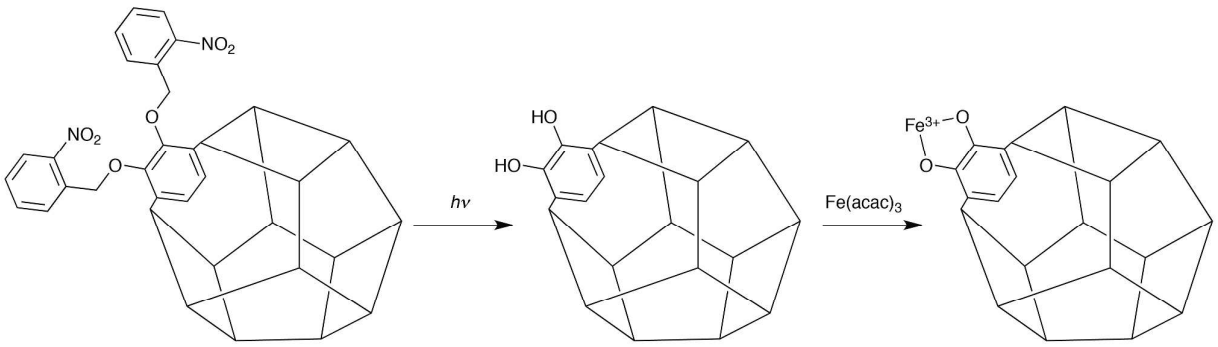

Figure 3. An example of post-synthetic photochemical deprotection of chelating catechol units in $(Zn_4O)_3(BDC\text{-}NH_2)_3(BTB)_4$.

Chelating hydroxy functional groups can also be accessed via in-situ deprotection of acetyl groups.[33, 34] This was exemplified in the work of Rankine *et al*.[34] where acetyl masked biphenyl-2,2′-diol organic links were deprotected, in-situ under standard solvothermal conditions and the availability of the diol chelating groups for PSMet was evidenced by treating the MOF with $CuCl_2$. The versatility of deprotecting masked hydroxy functional groups for PSMet was recently outlined by Nguyen and co-workers.[35] In their work three protecting group strategies were independently applied - *o*-nitrobenzyl (photolabile), *tert*-butyldimethysilyl (chemically labile) and *tert*-butoxycarbonyl (thermally labile) - to mask a catechol secondary functional group that was an intrinsic component of the organic building unit. Of these three approaches the thermally labile *tert*-butoxycarbonyl was found to be the most efficient and least destructive to the framework structure. Subsequently, PSMet was carried out on the naked catechol groups with $VO(acac)_2$ to afford a catalytically active MOF.

MOFs comprised of coordinatively unsaturated metal nodes provide opportunities for grafting metal ligating moieties to the network architecture. For example, free coordination sites can be accessed at the chromium clusters of MIL-101 by removing bound solvent molecules under vacuum at 423 K.[36] The resulting Lewis acidic sites have been used to graft ethylene diamine affording pores with free primary amine groups.[37] These amines were used to facilitate PSMet with $PdCl_4^{2-}$ then subsequent reduction to form Pd nanoparticles. Additionally, the aluminium-based MOF MIL-53 is also amenable to post-synthetic modification at the metal node.[38] This was elegantly illustrated by Fischer and co-workers[39] who utilized the bridging hydroxide in the metal node to effect a ring opening reaction of 1,1′-ferrocenediyl-dimethylsilane, thus anchoring a ferrocene unit into the MOF pores. This technique has also been used effectively to graft dopamine to the metal oxide units of MIL-101.[40] Here, free catecholate groups of the dopamine moiety were found to bind $VO(acac)_2$. In addition, it was also demonstrated that protecting the catechol moiety of dopamine with sterically demanding tert-butyldimethyl silyl (TBDMS) groups restricted this post-synthetic anchoring to the surface of the MOF.

2.1.3 Addition of a metal via link substitution

Recently, post-synthetic exchange of organic framework components (Scheme 2e) has been used to facilitate PSMet by incorporating metalated links into the molecular backbone of the MOF.[41, 42] In such examples the metalated link possess identical structure metrics and primary functional groups to those that comprise the parent MOF; thus exchange occurs without disrupting the underlying framework topology. An important aspect of these studies is that 'linker-exchange' has been demonstrated in MOFs that are considered structurally robust.[42, 43] Preliminary studies were reported by Cohen *et al*. who demonstrated post-synthetic ligand exchange processes in two robust MOF materials, MIL-53(Al) and MIL-68(In). Building on this work the groups of Cohen and Ott added a molecular proton reduction catalyst into the highly robust Zr(IV)-based UiO-66 MOF by post-synthetic exchange of the organic links. Simple treatment of UiO-66 with the synthesised pre-catalyst link in deoxygenated ultrapure water at room temperature for 24 hours gave the metalated MOF. Conversion was estimated at approximately 14% by energy dispersive X-ray (EDX) analysis, integrity of the catalyst link shown by X-ray absorption spectroscopy and permanent porosity was shown to be maintained. Notably also, direct solvothermal synthesis fails to produce the functionalized MOF. The 'linker exchange' approach extolled here shows great potential as well-understood, well characterised and functionally-complex metal systems can be successfully introduced into the MOF pore network in one step with minimal impact on the structure. One consideration however is the size of the moiety with respect to the pore dimensions of the MOF but reticular chemistry design principles[4] can be used to overcome such challenges.

2.1.4 PSMet addition by formation of organometallic entities

The substantial organic component of MOF architectures has motivated researchers to explore the organometallic chemistry of the molecular backbone. Due to the significant reactivity of organometallic precursors PSMet has proven an excellent strategy for pursing such investigations (Scheme 2f). For example, Long *et al.* showed that the phenyl units of MOF-5 could be used to anchor an organometallic chromium complex (Figure 4).[44] Diffusing $Cr(CO)_6$ into the MOF-

5 pore network and heating to 140˚C gave rise to a (bdc)$Cr(CO)_3$ organometallic species (H_2bdc = 1,4-benzenedicarboxylic acid). Further, one of the CO ligands could be subsequently replaced by N_2 and H_2, respectively, via photolysis. A noteworthy conclusion of this work is that the rigid MOF architecture could be used to isolate and stabilise reactive organometallic species that were hitherto only accessible via gas phase, super-critical fluids or frozen matrices. In a later study, the effectiveness of MOFs as scaffold for isolating such organometallic species was reported by Bordiga and co-workers. In this case a thorough examination of incorporation of the $Cr(CO)_3$ moiety in UiO-66 was described.[45]

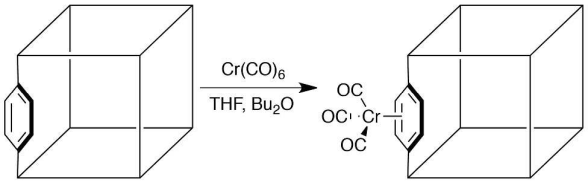

Figure 4. PSMet addition by formation of organometallic chromium complex as demonstrated in MOF-5.

Another example where the organic strut supports post-synthetic organometallic chemistry was reported by Mulfort *et al*.[46] In this case *N,N'*-di-(4-pyridyl)-1,4,5,8-naphthalenetetracarboxydiimide (dpntc) links were chemically reduced with Li^0 to presumably form dpntc+Li^+. Although comprehensive characterization proved elusive, this work showed that PSMet could be performed using strong reductants with maintenance of permanent porosity. Recent work by Dau *et al*. demonstrated the first post-synthetic cyclometalation reaction on a MOF framework.[47] Here MOFs constructed from 2-phenylpyridine-5,4'-dicarboxylic acid were post-synthetically treated with the cyclometalating agents $[Ir(COD)(OCH_3)]_2$ and $[Rh(COD)(Cl)]_2$, respectively. It was observed that for one of the interpenetrated MOFs studied in this work inter-framework interactions engendered remarkable site-selective cyclometalation. Given that organometallic species of second and third row transition elements feature prominently in homogeneous catalysis this work represents an important first step towards developing novel organometallic heterogeneous catalysts. For example, a similar approach has been employed by Lin *et al*. to develop water oxidation catalysts.[48]

Another route to achieving metal-free binding sites within a MOF is to utilize azolium containing linkers appended with heterocyclic or carboxylate primary donors. By judicious choice of reaction conditions azolium sites can retained in

the MOF[49] although often these have been inaccessible for PSMet or the strong bases required to deprotonate the azolium have been detrimental to the MOF structure. Wu and colleagues reported two MOFs formed from a double azolium linker that could be PSMet with $Pd(OAc)_2$ in THF.[50] For the more open 2D MOF ICP-MS demonstrated approximately 76% of azolium sites were post-synthetically metalated, while Transmission Electron Microscopy (TEM) and X-ray Photoelectron Spectroscopy (XPS) data were consistent with divalent Pd. Although the exact chemical form of the PSMet site was not established, the PSMet MOF catalyzed Suzuki-Miyura coupling reactions. Further to this work, Wu *et al*. synthesised a metal–organic nanotube material with an interlocked 3D structure.[51] Large channels in the honeycomb network (~3.3 nm) provide efficient access to a similar bis-azolium site which is ripe for PSMet. This was effected by treating the material with $Pd(OAc)_2$ in THF and the extent of metalation quantified by digestion experiments, XPS, TEM and inductively coupled plasma mass spectrometry (ICP-MS).

2.2 PSMet by metal or cation exchange

The development of frameworks possessing exchangeable charged entities attached to the framework structure or located within the pore network of the MOF has facilitated PSMet by exchange. Examples included PSMet by two approaches, exchange of metals coordinated to organic linkers (Scheme 3a) and exchange of extra-framework cations (Scheme 3b). Recently, access to anionic MOFs possessing particularly large pore apertures as enabled the examination of exchange of extra-framework charge-balancing cations by cationic metal complexes of significant sizes (Scheme 3b). Post-synthetic metal cation exchange of this type has been shown to enhance the performance characteristics of the parent MOF for applications, including gas adsorption,[52, 53] drug release,[54] and luminescence.[55, 56]

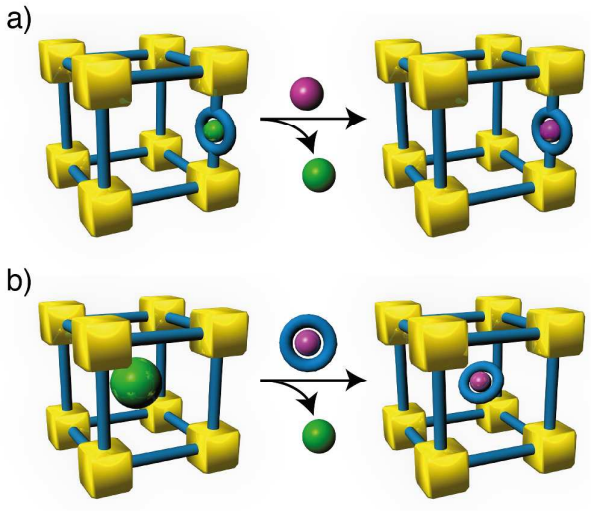

Scheme 3. PSMet by exchange of (a) metals or cations attached to organic linkers or (b) PSMet exchange of charge-balancing cations within the pore network by metal cations or cationic metal complexes.

2.2.1 Metal exchange of coordinated cations

An early example of exchanging non-structural metals in MOFs was described by Dincă *et al.*[57] (Figure 5) where the intra-framework Mn ions in the tetrazolate based MOF, $Mn_3[(Mn_4Cl)_3(BTT)_8(CH_3OH)_{10}]_2$, were post-synthetically exchanged with a variety of transition ions (Fe^{2+}, Co^{2+}, Ni^{2+}, $Cu^{2+/+}$, Zn^{2+} and the alkali metal Li^{+}). This PSMet via exchange was carried-out by immersing the parent MOF in concentrated anhydrous MCl_x, (x = 1 or 2), solutions over a period of a month. Here the gentle reaction conditions gave rise to metal-exchanged frameworks that maintained their structure and porosity. Further, this work clearly demonstrated the potential of ion exchange as a means of incorporating a wide variety of metal species into a given MOF pore network.

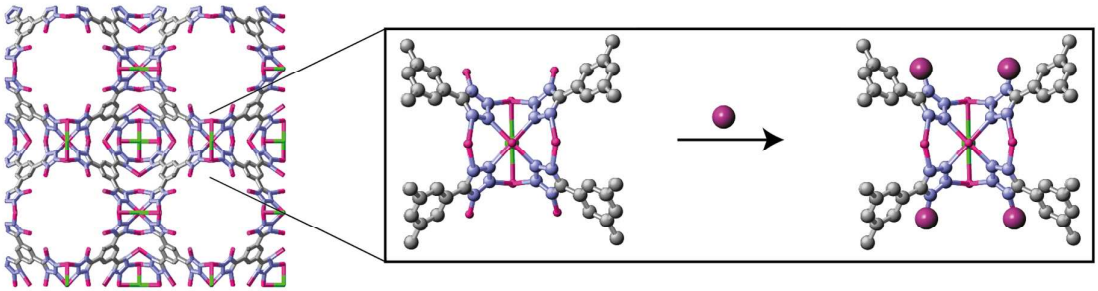

Figure 5. Exchange of non-structural metals in the tetrazolate based MOF, $Mn_3[(Mn_4Cl)_3(BTT)_8(CH_3OH)_{10}]_2$. The MOF structure (left) viewed down the *a*-

axis and a schematic of the PSMet exchange of non-structural Mn of the SBU (inset). The introduced metal is represented by a purple sphere while in the stick/ball and stick images, grey = carbon, blue = nitrogen, green = chlorine, pink - manganese.

Exchange of metal cations bound to framework links is another effective PSMet strategy. A salient example was reported by Ngyuen *et al.* who synthesized a pillared MOF comprised of dipyridyl Mn(salen) struts (Figure 6).[58] The Mn metalated salen link was selected as it allowed the predictable synthesis of the parent pillared MOF; it was noted that other metal ions obstructed MOF synthesis. PSMet was accomplished by first demetalating the Mn ion from the salen binding unit by treating the MOF with H_2O_2. It is worth noting that this demetalation strategy had been successfully employed by these authors to selectively 'demanganate' salen struts on the surface of a structurally similar Mn-salen pillared MOF.[59] The demetalated MOF was then PSMet with first row transition metal ions Cr, Co, Mn, Ni, Cu, and Zn by immersing the MOFs in the respective metal salt solution. Such approaches are akin to the PSMet addition strategies outlined in Section 2.1 utilising an orthogonal protecting groups; here the protecting group is a coordinated metal centre.

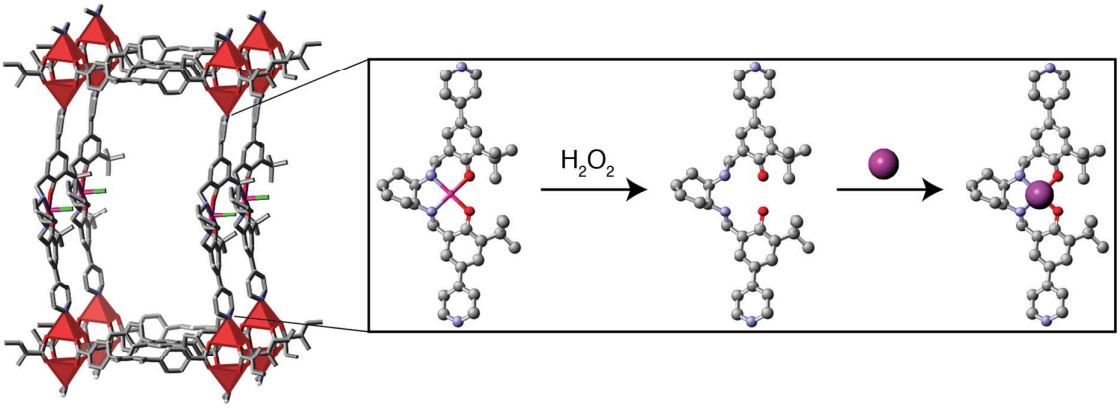

Figure 6. The post-synthetic demetalation and PSMet strategy of Ngyuen *et al.* in a pillared MOF comprised of dipyridyl Mn(salen) struts. A view of one cage of the MOF structure (left) and the demetalation/PSMet procedure of an isolated Mn(Salen) strut is shown in the inset. In the images grey = carbon, blue = nitrogen, red = oxygen, green = chlorine, pink = manganese, and the red square-based pyramids show the coordination environment of the zinc(II)-based

paddlewheel nodes. First row transition metal ions, added by PSMet, are represented by a purple sphere.

Exchange of metal cations within a MOF linker has also been demonstrated for porphyrin links. For example, Ma *et al.*[60] post-synthetically substituted Cd^{2+} with Co^{2+} in porphyrin links by heating the MOF in a DMSO solution of $Co(NO_3)_2$. Zaworotko and co-workers were able to perform metal exchange reactions on porphyrin molecules simply held in the MOF pores by electrostatic interactions.[61] In this example the porphyrin-bound Cd cations were replaced with Mn and Cu by treating the MOF with the respective metal salts. Metal exchange at the SBU was also observed for Mn (100%) and Cu (76%) after one month compared with approximately 7 days for exchange of the Cd cation in the porphyrin.

2.2.2 Metal exchange of pore encapsulated cations

PSMet via ion exchange has also been described by Eddaoudi and co-workers in *rho*-ZMOF architectures[62] and Lu *et al.* in lanthanide based frameworks[63] where extraneous alkali, alkali earth and second and third row transition metal cations were substituted into the frameworks. In work reported by Eddaoudi pertaining to DMA-*rho*-ZMOF, which could be prepared from 4,5-imidazoledicarboxylic acid and $In(NO_3)_3{\cdot}2H_2O$, dimethylammonium cations formed during synthesis (from DMF) could be substituted by sodium, lithium and magnesium cations. Interestingly, the lithium containing framework had to be prepared in two steps with initial exchange by sodium followed by lithium. The location of these aquated extra-framework cations was identified by single crystal X-ray diffraction to be a hydrogen bond acceptor pocket generated by carboxylate groups from four molecules of the 4,5-imidazoledicarboxylate ligands.

Work based on an analogous MOF to the one described in Section 2.2.1 outlining a novel PSmet approach to introducing metal cations into MOF pores was recently reported by Zaworotko and co-workers.[64] In this example a Cd based MOF was synthesized that encapsulated cationic porphyrin moieties via supramolecular interactions within its pore structure. The porphyrin guests were observed to bind Cd ion in square pyramidal geometry with an axially co-ordinated solvent molecule. Immersing the MOFs in either $BaCl_2$ or NaCl was

found to exchange the solvent molecule for a chloride anion while the cations are bound by carboxylate groups of one of the metal paddlewheel units. Interestingly, Cd and Mn salts could be added to the framework via a similar mechanism in which surprisingly neither metal was shown to displace the Cd^{II} centre coordinated by the porphyrin. While this approach is not strictly ion exchange it does represent a unique approach to incorporating extraneous metal cations into the pores.

MOFs can be readily synthesized with pore sizes several nm in diameter.[65] As a consequence, in addition to solvated metal ions, charged metal complexes can also be introduced into MOF pore networks via ion exchange. For example, the yellow light emitting iridium complex $[Ir(ppy)_2(bpy)]^+$ (Hppy = 2-phenylpyridine, bpy = 2,2'-bipyridine) was diffused into the mesoporous network of the cadmium based anionic MOF, $[(CH_3)_2NH_2]_{15}[(Cd_2Cl)_3(TATPT)_4]\cdot 12DMF\cdot 18H_2O$ (TATPT = 4,6-tris(2,5-dicarboxylphenyl-amino)-1,3,5-triazine).[66] The molecular size of $[Ir(ppy)_2(bpy)]^+$, approximately 10 × 11 Å, rendered it small enough to pass though the pore windows of the MOF which measured up to 15.5 × 15.5 Å. Accordingly, using DMF solutions, the iridium complex was diffused into the pores of the MOF at up to 8.8% loading with respect to Cd. Sanford and co-workers employed a similar exchange strategy and showed that organic, $NH_2Me_2^+$, cations could be partially exchanged within the pores of ZJU-28[67] with a variety of charged transition metal catalysts, including $[Pd(CH_3CN)_4][BF_4]_2$, $[FeCp(CO)_2(thf)]BF_4$, $[Ir(COD)(PCy_3)(py)]PF_6$, $[Rh(dppe)(COD)]BF_4$, and $[Ru(Cp^*)(CH_3CN)_3]OTf$.[68] These examples highlight that ion exchange of cations within MOFs is a facile method for encapsulating molecular compounds of predetermined function within the pore network. The scope for designing novel functional materials using this approach is vast as the structure metrics of the host framework can, in principle, be intimately modified to accommodate broad range of guests.

2.3 Pore Encapsulation

The pore networks of MOF materials are an ideal host matrix for the encapsulation of various metal-based guest moieties. The metal-containing moieties introduced in this manner include organometallic species, precursors

for chemical vapour deposition, nanoparticles, polyoxometallates and even metalloenzymes. Scheme 4 delineates the main strategies that have been employed, including (a) guest introduction, (b) nanoparticle formation and (c) 'ship-in-a-bottle' self-assembly.

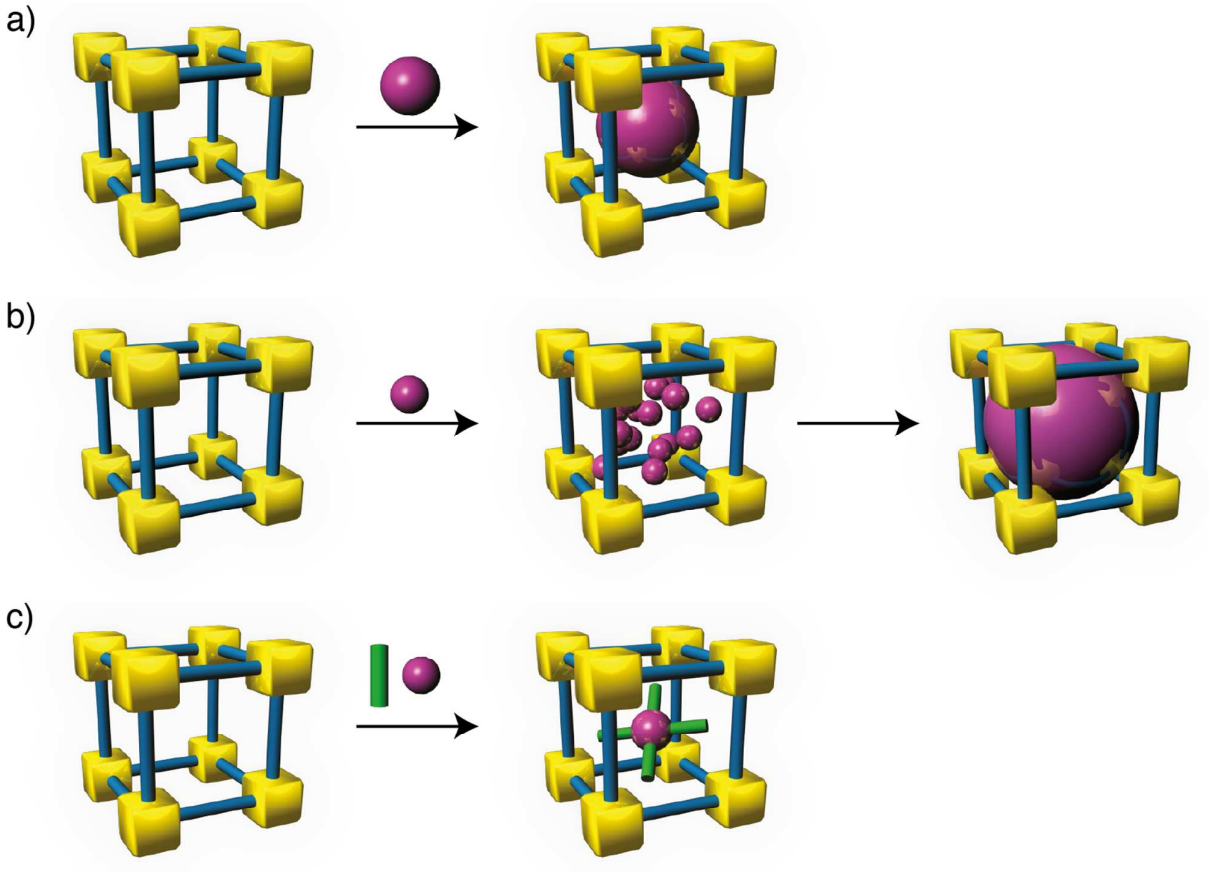

Scheme 4. Strategies that have been employed to encapsulate neutral metal-containing species, including (a) guest introduction, (b) nanoparticle formation from molecular precursors and (c) 'ship-in-a-bottle' self assembly.

2.3.1 Encapsulation of metal species within MOF pores

An obvious PSMet strategy for MOFs is to encapsulate metal species as guests within their expansive pore networks. In such cases the MOF architecture can act as a matrix to control the relative positions of metal compounds, or metal clusters/nanoparticles in 3D space. Experimental data has shown that metal species can be diffused into the pores in solution or vapour phase or, alternatively, the metal complex or cluster can be post-synthetically synthesized within the framework pore cavity. Early work in this area by Kim *et al*. used vapour phase diffusion methods to infiltrate the pores of MOF-5 with

ferrocene.[69] This method proved very efficient resulting in a loading of seven molecules of ferrocene per pore thus leaving only 1.6% of the crystal volume solvent accessible. In this case, the high loading facilitated characterisation of Fc@MOF-5 by X-ray diffraction methods using synchrotron radiation. Fischer and co-workers also demonstrated that organometallic species could be loaded into the pores using vapour phase methods.[70] Common metal-organic chemical vapour deposition precursors for a variety of metals (Fe, Pt, Pd, Au, Cu, Zn, Sn) were reversibly loaded into the pores of MOF-5 without observed structural decomposition of the host framework. The high efficiency of this methodology has underpinned a body of work[71] investigating the in situ formation of metal and metal oxide nanoparticles within MOFs (see section 2.3.2).

MOFs can possess large pore networks that are suitable for encapsulating nanometre-sized metal-oxide clusters such as polyoxometallates. For example, the sizeable pores of CrMIL-101 were shown to accommodate $K_7PW_{11}O_{40}.nH_2O$ after being treated with a solution of the salt for 2 hours (Figure 7).[72] Kholdeeva and colleagues also prepared composite materials based on the MIL-101 matrix but with the encapsulation of redox active Keggin heteropolyanions,[73] $[PW_{11}CoO_{39}]^{5-}$ and $[PW_{11}TiO_{40}]^{5-}$ and polyoxotungstates,[74] $[PW_4O_{24}]^{3-}$ (PW4) and $[PW_{12}O_{40}]^{3-}$ (PW12). Synthesis was accomplished by addition of starting material salts to a stirred suspension of the MOF. The catalytic performance of these materials for the oxidation of alkenes was explored.

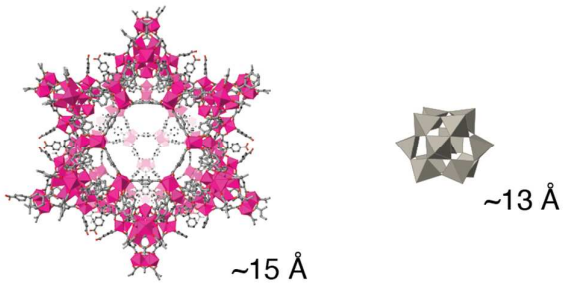

Figure 7. A representation of one cage of the CrMIL-101 structure (left) viewed down one of the 15 Å pore windows. The chromium nodes of the structure are shown as pink polyhedra. The polyoxometalate $PW_{11}O_{40}^{7-}$ structure (right) provides some idea of the relative pore window size of CrMIL-101 and the van der Waals size of POM.

Recent work by Ma and co-workers[75] demonstrated the remarkable capacity of MOF materials to encapsulate metal-containing biomolecules. Here a mesoporous MOF framework could be post-synthetically metalated by encapsulation of the heme containing microperoxidase-11 (MP-11). This was achieved by immersing the mesoporous Tb-based MOF in a solution comprised of MP-11 and HEPES (4-(2-hydroxyethyl)-1-piperazineethanesulfonic acid) buffer at 37˚C resulted in a loading of 19.1 μmol/g.

2.3.2 Nanoparticle encapsulation

Post-synthetic incorporation of metal nanoparticles into MOF architectures holds great promise for controlling the size and spatial distribution of nanoparticles without direct surface passivation. PSMet strategies of loading metal nanoparticles into MOF pores include vapour deposition of volatile metal-organic precursors followed by reduction, wet chemical methods or solid state grinding.[76, 77] One of the first examples of metal nanoparticles in MOFs, described initial vapour phase loading of MOF-5 with the organometallic precursors [(η^5-C_5H_5)Pd(η^3-C_3H_5)], [(η^5-C_5H_5)Cu(PMe_3)] and [(CH_3)Au(PMe_3)].[78] Subsequent reduction by H_2, and concomitant thermal treatment for [(CH_3)Au(PMe_3)], afforded M@MOF-5 (M = Au, Cu, and Pd) composites. It is noteworthy that for Cu@MOF-5 and Au@MOF-5 the long range order remained intact, however for Pd@MOF-5 the PXRD pattern suggested a distinct loss of crystallinity. Nevertheless, the surface area (Langmuir) of Pd@MOF-5 remained relatively high at 1600 m^2g^{-1}. According to XRD and TEM data the nanoparticle size ranges for M@MOF-5 were 1.4 nm +/-0.1 (Pd) , 3-4 nm (Cu) and 5-20nm (Au). The large size of the gold nanoparticles was attributed to the mobility throughout the pore network leading to agglomeration at the materials surface. Using analogous methodology Fischer and co-workers demonstrated the generation of a variety of other metals NPs within MOFs including Ru,[79] and TiO_2.[80] Such studies indicate the broad scope of this technique and provide access to platforms that enable the properties of nanoparticles to be exploited.

The introduction of metal nanoparticles in MOFs can also be accomplished via solution methods where a metal precursor is diffused into the pore cavities and reduced in situ. For example, Ferey and co-workers diffused $PdCl_4^{2-}$ into the pores of amine functionalised CrMIL-101 followed by reduction with $NaBH_4$ to

afford Pd nanoparticles.[81] The protonated amine functional groups were reported to facilitate encapsulation of the precursor salts and ultimately support anchoring of the nanoparticles. A similar approach was employed Matzger and co-workers[82] who demonstrated how creating framework defects affords free carboxylate functional groups in the pores of a new material termed MOF-5(O_h). The defects in this novel MOF are engendered by adding small amounts of H_3BTB to a standard MOF-5 synthetic procedure resulting in an octahedral MOF-5 structure. Addition of $Pd(OAc)_2$ to the MOF-5(O_h) pores led to a 2.3 wt % loading of Pd, which was attributed to the interaction between Pd and the free carboxylate groups. PXRD and gas adsorption isotherm studies determined that the Pd loaded MOF maintained its structural order and high porosity 2600 m^2g^{-1}. Treating the Pd(OAc) loaded MOF-5(O_h) crystals with $NaBH_4$ resulted in reduction of the Pd(II) species to Pd nanoparticles. TEM studies confirmed an even distribution of Pd nanoparticles throughout the MOF and, remarkably, the surface area of the Pd nanoparticle MOF remained essentially identical (2570 m^2g^{-1}) along with retention of long range order. This work exemplifies how creating defect sites can lead to enhancing the uptake of extraneous metals in MOF pores (Pd uptake in MOF-5 was found to be insignificant). The post-synthetic introduction of metal nanoparticles is a rapidly expanding area and here we have highlighted some prominent strategies that have been employed to incorporate these extraneous metals into the pore network of MOFs. A more comprehensive description of the variety of strategies and characterisation methods applied to these materials has been recently reviewed elsewhere.[77]

2.3.3 Constructing metal species inside pore cavities

A novel PSMet strategy was recently reported by Das and co-workers where the binuclear manganese catalyst [(2,2':6',2"-terpyridine)Mn(μ-O)$_2$Mn(2,2':6',2"-terpyridine)]$^{3+}$ (MnTD) was post-synthetically constructed within the mesopores of CrMIL-101.[83, 84] The structural dimensions of MnTD are too large to allow diffusion through the pore windows of CrMIL-101 however it is small enough to fit within the giant pore cavities. Accordingly, a 'ship-in-a-bottle" approach was employed which afforded 10wt% MnTD loading, equivalent to one MnTD molecule per pore cavity. Such strategies have been used in zeolite chemistry where structure topologies commonly yield materials with relatively small pore windows with respect to their cavity size[85] and may hold promise for further

investigation in MOFs as more complex metal-based guests are targeted. Along similar lines Ma *et al.*[86] described the synthesis of a Co phthalocyanine complex (Co-Pc) within the pores of Bio-MOF-1 ($Zn_8(ad)_4(BPDC)_6O\cdot 2Me_2NH_2$, where ad = adenine).[55] Bio-MOF-1 has 1D channels possessing $Me_2NH_2^+$ cations which can be readily exchanged for metal ions. By effecting exchange of $Me_2NH_2^+$ cations for Co^{II} (*ca.* 85% exchange) and subsequently treating the MOF in a formamide solution of 1,2-dicyanobenzene at 190°C for 10 minutes Co-Pc was formed (*ca*. 30% conversion) within the structure of Bio-MOF-1 (i.e. Co-Pc@Bio-MOF-1). This was confirmed visually by an intense blue colouration of the normally colourless Bio-MOF-1 crystals and by comparison of solid-state UV-visible absorption spectra for Co-Pc@Bio-MOF-1 and Co-Pc. In a similar manner Ni-Pc@Bio-MOF-1 and Cu-Pc@Bio-MOF-1 were formed and the performance of all three materials examined for the epoxidation of styrene.

3 Applications

The primary aim of PSMet is to enhance a particular physical property of the parent MOF or imbue the framework with an entirely new performance characteristic. The previous section outlined the abundance of established strategies for PSMet of MOFs and thus highlights the rich palette at hand for designing porous materials with pre-determined properties. Accordingly, post-synthetically metalated frameworks have been widely applied in areas where their porous nature can be effectively utilized such as heterogeneous catalysis and selective gas adsorption. Rather than comprehensively surveying all the known examples of PSMet and its applications, the following section seeks to describe some salient studies where the rational design has led to a significant impact in the field of MOFs or indeed solid-state chemistry. It is anticipated that this approach will provide the reader with a grasp of the expansive scope of this technique for generating tailored functional materials and the applications of such materials.

3.1 Catalysis

Metal ions and clusters play a significant role in both homogeneous and heterogeneous catalytic processes. As a result, many of the applications of PSMet in MOFs are directed towards improving the stability, efficiency or performance of catalytic reactions of potential commercial interest. Given the vast number of reports of catalytic activity in post-synthetically metalated MOFs, rather than

highlight proof-of-concept reactions, we will elaborate on some salient examples where PSMet has been employed in a pre-determined approach towards the design of novel catalysts.

The building block approach to MOF synthesis offers great potential for constructing recoverable and selective asymmetric catalysts. Lin and co-workers recently described a series of asymmetric catalysts generated by PSMet of a dihydroxy chelating group that is part of a chiral framework.[87] The MOF catalysts described in this work were constructed from organic links based on an enantiopure 4,4',6,6'-tetracarboxcylic acid functionalised BINOL moiety and a PSMet step was required in order to incorporate a catalytically active Ti^{IV} ion into the pores. These catalysts were shown to be very effective at catalysing the reduction of a variety of ketones to chiral secondary alcohols. PSMet formed a critical part of the design of these chiral MOF catalysts and clearly showed the utility of this technique for developing novel catalysts. Organometallic entities are well known catalysts and Cohen *et al.*[88] have used MOF platforms containing 5,4'-phenylpyridinedicarboxylic acid to introduce cyclometallated Ir catalysts into the framework by treatment of the parent materials with $[Ir(COD)(OCH_3)]_2$ (COD = 1,5-cyclooctadiene). These catalysts were used in C-N bond forming reactions, and were shown to be more stable in ambient conditions with a greater storage life than their molecular equivalents.

A different PSMet approach to engineering MOF catalysts was recently described by Sanford and co-workers.[68] In this example ion exchange was employed to infiltrate MOF pores with homogeneous transition metal catalysts (Figure 8). This elegant strategy is extremely versatile as the guest metal complexes are occluded within the MOF by non-specific electrostatic interactions. Accordingly, a wide variety of complexes can be incorporated into a single host framework. To this end a series of metal complexes, $[Pd(CH_3CN)_4][BF_4]_2$, $[FeCp(CO)_2(thf)]BF_4$, $[Ir(COD)(PCy_3)(py)]PF_6$, $[Rh(dppe)(COD)]BF_4$ and $[Ru(Cp^*)(CH_3CN)_3]OTf$, were partially exchanged with $Me_2NH_2^+$ organic cations that were located in the pores of the MOF ZJU-28. In each case approximately 30% of the organic cations were replaced by PSMet. The capacity of these materials to act as heterogeneous catalysts was assessed by selecting [Rh(dppe)(COD)]@ZJU-28 as a case study for the catalytic reduction of 1-octene. Acetone solutions of 1-octene were treated with 0.2 mol% of [Rh(dppe)(COD)]@ZJU-28 and the homogeneous catalyst

[Rh(dppe)(COD)]BF_4, respectively and placed under 10 atm of H_2. After 4hrs each catalyst performed approximately 450 turnover or essentially complete conversion of 1-octene. However, the advantage of the heterogenized catalyst was that it could be recycled 4 times under the same reaction conditions whereas the homogeneous counterpart performed poorly after recycling, completing only 200 further turnovers after a further 500 equiv of the alkene were added after 4 hrs. Clearly the host framework stabilized the rhodium catalyst thus substantially increasing its overall efficiency. PSMet via ion exchange shows great promise for generating MOF based catalysts given the facility that a wide range of preformed homogeneous catalysts can be infiltrated into the MOF pores. Notably, as this example shows, these catalysts do not have to be anchored to the MOF framework to minimise leaching or benefit from stabilising benefits of inclusion. Additionally, the isoreticular principle will allow researchers to extend such work to studying the effect on pore size and shape on the efficiency of guest metal based catalysts. The PSMet strategies hitherto reported in the literature point to a bright future for guest metal catalysts, especially given the plethora of promising homogenous systems that can be identified for such investigations.

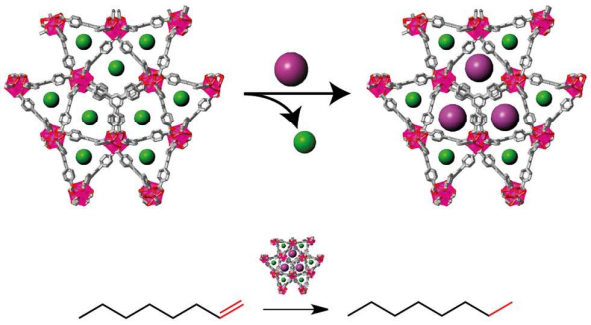

Figure 8. PSMet by exchange within the pores of ZJU-28 leading to a [Rh(dppe)(COD)]@ZJU-28 catalyst which catalyses the reduction of 1-octene to octane. The organic cations of the parent framework are represented by green spheres and the location of the catalytic metal complexes shown by purple spheres.

Pullen *et al.*[42] recently employed linker exchange as a means of introducing a preformed catalyst into the pores of a MOF. One of the key aspects of this work is based on earlier studies from the Cohen group who demonstrated that linker exchange could be carried-out on what are considered chemically robust

frameworks.[43] In this study a proton reducing catalyst [FeFe](dcbdt)$(CO)_6$ (dcbdt = 1,4-dicarboxylbenzene-2,3-dithiolate), of the same structure metrics and primary functionality as the links of the parent MOF, was incorporated into the molecular architecture of the MOF via a PSMet linker exchange process (Figure 9). This preformed binuclear iron catalyst was introduced into the framework of the well-known and chemically robust framework, UiO-66.[7] When part of a photochemical system, including the photosensitizer $[Ru(bpy)_3]^{2+}$ and ascorbate as an electron donor, [FeFe](dcbdt)$(CO)_6$ functionalised UiO-66 was found to significantly outperform its homogeneous counterpart, [FeFe](dcbdt)$(CO)_6$, with respect to hydrogen production. Furthermore, control experiments clearly showed that the parent zirconium framework did not contribute to H_2 evolution. This approach shows that PSMet via linker exchange can give rise to complex functional systems. Moreover, given that the metal complex is incorporated into a well-defined matrix, structural characterisation will be facilitated which will undoubtedly provide valuable insight into these hybrid systems.

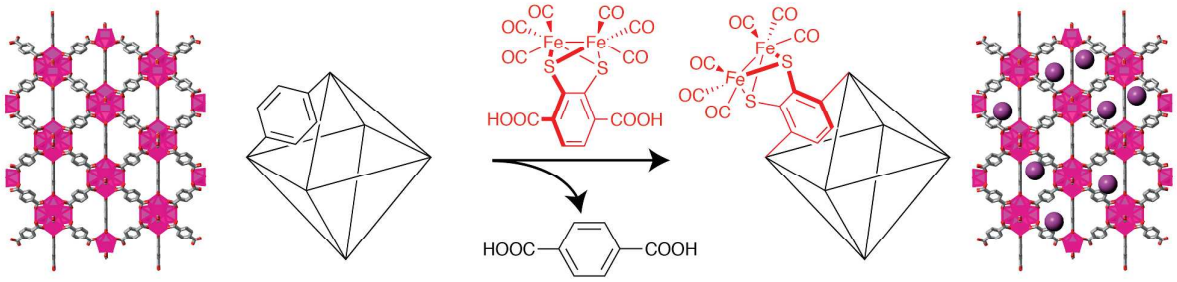

Figure 9. Developing advanced catalytic systems by direct linker exchange in UiO-66 with a preformed catalyst. The MOF structure (left, carbon = grey, oxygen = red, and the zirconium metal centres of the nodes as pink polyhedra), the chemistry of the PSMet step (centre) and a representation of the [FeFe](dcbdt)$(CO)_6$ functionalised UiO-66 material (right, the purple sphere represents the [FeFe](dcbdt)$(CO)_6$ entity).

Recent work by Ma and co-workers described a novel PSMet strategy that involved diffusing the metalloenzyme microperoxidase-11 (MP-11) into the pore cavities of a mesoporous framework.[75] Given that another recent example of protein inclusion in MOFs has been reported,[65] this approach may have potential scope for taking advantage of the high selectivity and efficiency of enzyme catalysts by stabilising them in MOF pore networks. MP-11 was diffused into the

pores of a Tb based mesoporous MOF by placing the solid MOF in a buffered solution of MP-11. Immobilisation of MP-11 within the pores of the Tb MOF was confirmed by spectroscopic and gas adsorption isotherm experiments. The motivation for isolating MP-11 within a porous matrix is due to the proclivity of the enzyme to aggregate in solution and to therefore operate with a significantly diminished catalytic efficiency. The catalytic competency of the MP-11 loaded Tb MOF was evaluated by measuring its efficiency for the oxidation of 3,5-di-*t*-butylcatechol to *o*-quinone. In comparison to free MP-11 (8.93×10^{-4} mM/s) the initial rate of conversion of the MOF immobilised enzyme was slightly lower at 3.57×10^{-5} mM/s, however, the overall conversion of 48.7% for the MP-11/MOF system far exceeded that of the free enzyme which was found to be 12.3%. This enhanced performance was attributed to stabilisation of the enzyme in the porous host. The effect of loading the enzyme in the porous silica material MCM-41 was found to be far less significant. The MCM41/MP11 material showed a slightly diminished initial rate (7.58×10^{-5} mM/s) with respect to the MOF-MP-11 system and a significantly diminished overall conversion of 17%. In addition the recyclability of the MCM-41 material was significantly poorer than the MOF-MP-11 MOF-enzyme conjugate. These differences in catalytic efficiency between the two porous hosts may be accounted for by guest leaching from MCM-41. The positive outcome of this work points towards further studies aimed at incorporating and stabilising catalytically competent metalloenzymes inside MOFs.

MOF topologies that afford large pore cavities and relatively small pore windows afford opportunities for ship-in-a-bottle synthesis of metal complexes. This approach essentially traps the guest within the pore network by preventing leaching by diffusion and can enhance the stability of reactive species by isolating them from the bulk solution. This strategy motivated Nepal *et al*. towards the PSMet of CrMIL-101 with a well-studied water oxidation catalyst by post-synthetic assembly within the framework. MnTD $[(terpy)Mn(\mu\text{-}O)_2Mn](terpy)]^{3+}$ is a reactive homogeneous water oxidation catalyst that primarily degrades via contact with other MnTD species in solution.[83, 84] Accordingly, by isolating this catalyst in the pores of a MOF sustained catalysis may be achieved. MnTd was assembled in the pores of Cr-MIL101, which is both chemically robust and is comprised of large pore cavities accessed via relatively small windows, by first diffusing terpy into the MOF followed by concomitant

addition of $Mn(OAc)_2$ and a stoichiometric amount of K-Oxone (potassium peroxomonosulfate). MnTD loaded Cr-MIL101 showed remarkable sustained oxygen evolution compared to that of free MnTD which was essentially deactivated after 400s. These exceptionally promising results demonstrate that this "ship-in-a-bottle" PSMet approach can be successfully employed for stabilising reactive homogeneous catalysts.

Metal and metal oxide nanoparticles are well known for their catalytic properties.[76, 77] MOFs have been employed as hosts for nanoparticles in an attempt to maximise their potential for catalysis through stabilisation in a porous host. Kaskel and co-workers have demonstrated that the inclusion of nanoparticles in MOFs can yield significantly increased catalytic activity for Pd nanoparticles. Specifically Pd@MOF-5 showed high reaction rates for the hydrogenation of styrene in comparison to Pd nanoparticles loaded on porous carbon.[89]

3.2 Selective Gas adsorption

The introduction of extraneous metal ions into the MOF pore network can have a significant effect on the surface potential and thus modulate adsorbate-surface interactions. Thus PSMet has been utilised as a strategy for enhancing the selective gas uptake of the parent framework in an analogous approach to the formation of open metal sites at the metal nodes.[90-92] However, a potential advantage of PSMet is that a variety of metal ions and pore sizes could be surveyed for their gas adsorption properties in a series of iso-reticular frameworks. Bloch and co-workers demonstrated that PSMet of a MOF replete with free bipy donors could improve the selective uptake of CO_2 over N_2.[9] In this case PSMet was carried out with both Pd and Cu respectively. In particular incorporation of $Cu(BF_4)_2$ in the pores significantly enhanced the affinity of the material for CO_2 and its total uptake capacity (Figure 10). The calculated selectivity increased by a factor of 4 and the isosteric heat of adsorption increased by approximately 30%. This work demonstrated how PSMet can be used to incorporate metal salts into the pores of a MOF material and how they can be effectively used to tune the performance characteristics of the material.

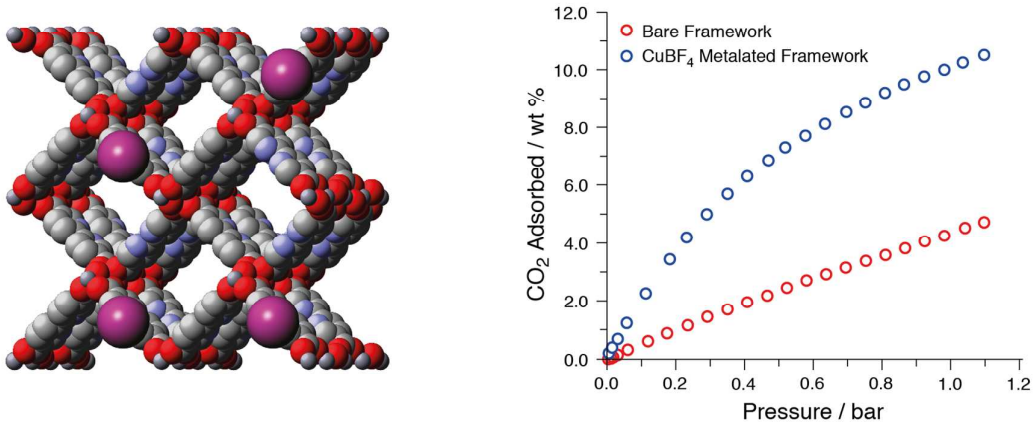

Figure 10. A structural representation of the MOF Al(OH)(bpydc)·0.97Cu(BF_4)$_2$ (left) and the CO_2 isotherms at 298 K (right) observed for the PSMet MOF Al(OH)(bpydc)·0.97Cu(BF_4)$_2$ (blue) compared with its parent MOF (red). In the MOF structure: grey = carbon, blue = nitrogen, red = oxygen, small grey sphere = aluminium, and the purple spheres show the locations of the copper centre (only a few sites shown but based on analysis 97% of sites are occupied).

PSMet can also be used to incorporate smaller more highly charged ions within MOF pores. The aim of introducing such moieties has particular application to hydrogen storage where it has been shown computationally that surface anchored cations with high charge density, e.g. Li^+, Mg^{2+}, could substantially increase H_2 affinity and uptake capacity at desirable temperatures and pressures.[93, 94] One of the challenges to be overcome in this area is the structural characterisation of the metalated MOF as this would provide deep insight into the adsorption process and provide pathways to designing more effective materials. Nevertheless, Hupp and co-workers[16] have demonstrated that PSMet incorporation of lithium into MOF pores can afford improvements in H_2 affinity and total uptake. In one approach the post-synthetic generation of lithium alkoxide moieties gave rise to a slight increase in H_2 uptake. It is worth noting that the affinity of the metalated material towards H_2 is dependent on the lithium loading. MOFs with higher lithium loadings showed diminished uptake with respect to their less metalated counterpart. This was attributed to framework degradation, however, as previously mentioned structural characterisation would provide valuable insight into these materials. Nouar *et al.*[62] showed that modulating the electrostatic field by PSMet ion exchange could also moderately increase the H_2 affinity. In this work the organic $Me_2NH_2^+$ cations within the

pores of an anionic framework were exchanged with Li^+ and Mg^{2+} to yield materials with isosteric heats of adsorption of 9.1 and 9.0 kJ/mol respectively, compared to 8 kJ/mol for the organic cations. The authors comment that the metal cations are most likely present in their hydrated forms thus direct M^+-H_2 interactions are unlikely. The versatility of PSMet for systematically studying gas uptakes was elegantly demonstrated by Dincă *et al*.[57] In this case $Mn_3[(Mn_4Cl)_3(BTT)_8(CH_3OH)_{10}]_2$, was post-synthetically exchanged with Fe^{2+}, Co^{2+}, Ni^{2+}, $Cu^{2+/+}$, Zn^{2+} and Li^+. This work showed that the isosteric heat of adsorption for H_2 varied from 8.5 kJ/mol for Cu^{2+} to 10.5 kJ/mol for Co^{2+}. It is noteworthy that the lithium ions showed relatively modest heats of adsorption of approximately 9 kJ/mol. This work clearly shows the effectiveness of the PSMet approach for systematically studying such systems.

Introducing Li^+ ions into MOFs via framework reduction showed considerable enhancement in the uptake capacity and isosteric enthalpy of adsorption for H_2. Indeed H_2 adsorption in $Zn_2(NDC)_2(diPyNI)$ (NDC = 2,6-naphthalenedicarboxylate; diPyNI = N,N-di-(4-pyridyl)-1,4,5,8-naphthalenetetracarboxydiimide) increased dramatically from 0.93 wt% to 1.63 wt%. At one atm this is equivalent to an additional loading of 60 H_2 molecules per Li. The authors attribute this increase to the presence of unsaturated Li ions in the framework, however, acknowledge that this dramatic increase cannot solely be ascribed to the metal ion and is likely associated with changes in the framework structure and polarizability.[46]

Thallapally and co-workers have shown that PSMet with silver naonparticles is an effective approach for enhancing the uptake of noble gasses in MOFs. Here MOF-74-Ni loaded with silver nanoparticles maintained its structure and surface area and showed a 15.6% increase in the uptake of Xe with respect to the parent MOF. It is noteworthy that this enhancement is achieved with a moderate Ag loading of 1.47%.[95]

3.3 Metal sequestration and sensing

MOFs primed for PSMet can also be used to sequester metals, which have obvious applications in the capture or sensing of precious or toxic metal ions. In this case optimising the metal uptake is the ultimate goal. The most successful strategies for enhancing post-synthetic uptake of metals has been to synthesise

MOFs that have a high density of metal coordinating moieties lining the framework backbone without completely diminishing the porosity. For example He *et al*. synthesised an open framework based on the MOF-5 topology from 2,5-dithioalloxyterephthalic acid.[19] The resulting framework was replete with allyl thioether functional groups that sequestered Pd through the allyl moieties. In addition the Pd species was also found to interact with the sulfur, perturbing conjugation and giving rise to a colour change from pale yellow to deep orange/red. It is noteworthy that when the MOF was immersed in solutions with as low as 0.5 ppm Pd, the guest metal could be visually detected. This significant colour change was only observed for Pd at such low concentrations and not for other metals, suggesting that this material may have potential for sequestration, separation and/or sensing of Pd. Free thiol groups have also been employed as a means of sequestering heavy metals.[20] Yee *et al*. demonstrated that constructing frameworks out of the thiol rich ligand 2,5-dimercapto-1,4-benzenedicarboxylic acid gave rise to a permanently porous framework with a high density of free thiol functional groups. A Zr based framework of UiO-66 topology was constructed from this sulfur rich ligand that showed significant Hg uptake from solution (Figure 11). Furthermore subsequent to Hg uptake the MOF retained its long ranger order. This work exemplifies that the stability of Zr frameworks in a variety of solvents renders it an ideal platform for occluding metal ions. Indeed Lin and co-workers show that a phosphorylurea functionalised Zr MOFs can be used to effectively extract UO_2^+ from water and simulated seawater. One example based on a MOF containing a diethoxyphosphorylurea group afforded a UO_2^+ uptake of 217 mg U g^{-1} of MOF.

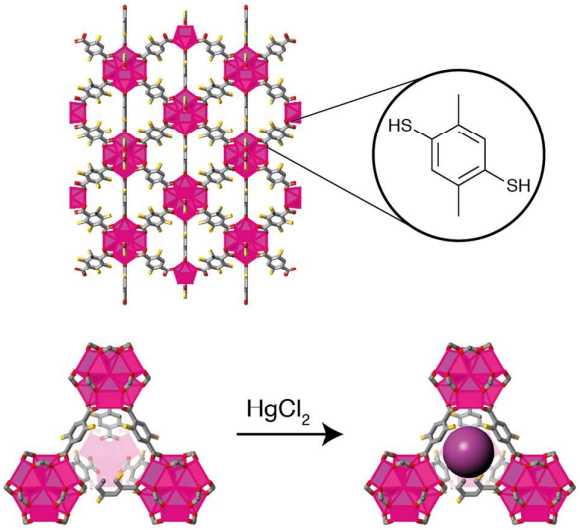

Figure 11. Hg uptake by PSMet in a thiol derivatised UiO-66 framework. The UiO-66 framework (top) with the inset showing the ligand, and the sulfur rich pore highlighted (below).

A mesoporous framework termed PCN-100 ($Zn_4O(TATAB)_2$ 317(DEF)33(H_2O) (H_3TATAB = 4,4',4"-s-triazine-1,3,5-triyltri-p-aminobenzoic acid) that possesses potentially chelating amine and azine donors, similar to the commonly employed aminopyridinato moieties, as an intrinsic part of its molecular backbone, was shown to be effective at sequestering heavy metals.[18] ICP studies demonstrated that PCN-100 effectively captured Cd^{2+} and Hg^{2+} from solutions highlighting its potential for heavy metal sequestration.

3.4 Light emission

Luminescence in MOF materials is a well-established property but most omit light of specific wavelengths related to the nature of the metal centres that constitute their nodes. Li and co-workers[66] utilised a PSMet strategy to generate a white light emitting MOF by encapsulating an iridium complex in the pore cavities of a mesoporous blue-emitting MOF; blue-emitting anionic MOF, $[(CH_3)_2NH_2]_{15}[(Cd_2Cl)_3(TATPT)_4].12(DMF).18(H_2O)$ (TATPT = 2,4,6-tris(2,5-dicarboxylphenyl-amino)-1,3,5-triazine). The parent MOF emits bright blue light (λ_{em} = 425 nm) which is attributed to the emissive organic TATPT linker. By taking advantage of the two types of large cages in the MOF, with the dimensions of approximate 2 and 3 nm, the cationic $[Ir(ppy)_2(bpy)]^+$ (Hppy = 2-phenylpyridine, bpy = 2,2'-bipyridine) complex in DMF was exchanged into the pores of the MOF. After 7 and 10 days soaking approximately 7.5 wt% and 8.8 wt% $[Ir(ppy)_2(bpy)]^+$ was encapsulated, respectively. $[Ir(ppy)_2(bpy)]^+$@MOF composites emit bright white light with good colour quality with a high quantum yield when excited at 370 nm. Notably, in the composite the emission of the Ir^{III} is shifted by comparison to the free complex. The PSMet strategy utilised here opens up a vista of new combinations of light emitting guests and MOFs that could be combined systematically to tune the properties and performance of energy-saving solid-state lighting materials with the sole requirement being MOFs of sufficiently sized pore apertures. Alternatively, 'ship-in-a-bottle' approaches could be examined.

Petoud, Rosi and co-workers[55] reported a PSMet exchange approach to forming luminescent MOFs utilising the bio-MOF-1 framework ($(Zn_8(ad)_4(BPDC)_6O.2Me_2NH_2.8DMF.\ 11H_2O$, where ad = adeninate; BPDC = biphenyldicarboxylate) previously developed.[54] Ln^{3+}@bio-MOF-1 materials were synthesised by post-synthetic cation exchange of bio-MOF-1 with Tb^{3+}, Sm^{3+}, Eu^{3+} and Yb^{3+}, with the Ln ions introduced using DMF solutions to give Ln^{3+}@bio-MOF-1. Lanthanide-centred excitation spectra recorded for the Ln^{3+}@bio-MOF-1 materials, that had been washed with nanopure water, revealed emission maxima at 545, 640, 614 and 970 nm for the four MOFs (Tb^{3+}, Sm^{3+}, Eu^{3+} and Yb^{3+}, respectively). These observations are particularly impressive as water effectively quenches lanthanide luminescence. Importantly, the strategy appears to be general with potential for bio-MOF-1 to protect Ln cations by acting as a host and sensitise a broad range of visible and NIR-emitting lanthanides in water. Notably the work reported the first example of a MOF that encapsulates and sensitises a NIR emitting Ln ion substantiating strategies to utilise some materials as biological probes or sensor components.

3.6 Drug delivery and imaging

The potential to construct MOFs of open architectures from bio-compatible building blocks renders them candidates for drug delivery systems. Rosi and co-workers[54] have employed bio-MOF-1 to demonstrate the first post-synthetic cation triggered release of drug molecules, in this case the antiarrythmia drug procainamide HCl. Utilising the anionic nature of their novel framework the authors were able to incorporate procainamide HCl into bio-MOF-1 at 0.22 g/g material (~3.5 procainamide molecules per formula unit; 2.5 encapsulated and 1 associated with the exterior of the crystals) after 15 days soaking without loss of crystallinity. A PSMet strategy was then targeted to facilitate release of the procainamide from the bio-MOF-1-drug composite (Figure 12). The drug-loaded bio-MOF-1 material was transferred to phosphate buffered saline (PBS, 0.1 M, pH 7.4) with a steady release observed over 20 hrs and complete release of procainamide after 72 hrs. The role of post-synthetic cation exchange was explored by repeating the same experiment in nanopure water which only gave *ca*. 20% release over a similar period.

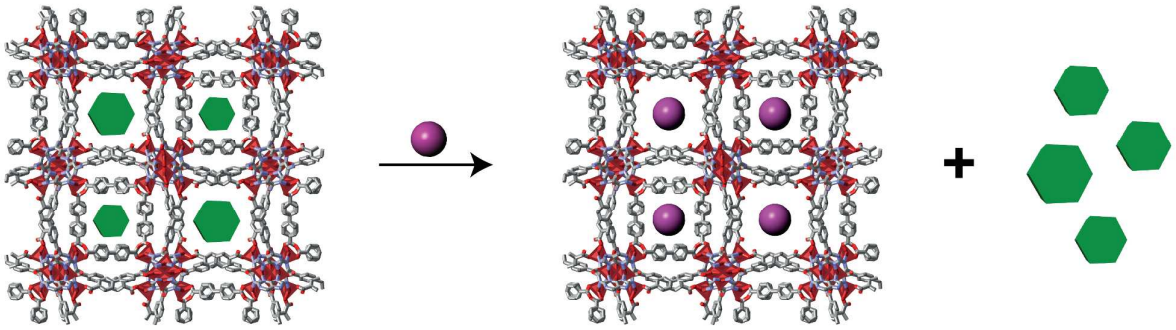

Figure 12. Utilising PSMet to trigger drug release. Bio-MOF-1 loaded with procainamide HCl was exposed to PBS buffer to induce cation exchange and drug release. Sodium ions are represented by purple spheres and drug molecules as green hexagons.

Analogues of the MIL family of MOFs[72] were used by Lin *et al*. to develop materials for imaging and drug delivery applications.[29] Fe containing MOFs ($Fe_3(\mu_3\text{-}O)Cl(H_2O)_2(L)_3$, where L = either pure BDC or mixtures of BDC and NH_2-BDC) were synthesised by the authors and shown to possesses an analogous structure to Cr-MIL-101 by PXRD. Based on this, two types of mesoporous cages with internal free diameters of ~29 and 34 Å were expected, making the amino functionalised material amenable to the loading of both imaging contrast agents and drug molecules. A covalent addition PSMet strategy was used to add a *cis*-platin prodrug into the pores of the Fe-MIL-101 structure. To achieve this the ethoxysuccinato-cisplatin (ESCP) prodrug, *c*,*c*,*t*-$[PtCl_2(NH_3)_2(OEt)(O_2CCH_2CH_2CO_2H)]$, was activated by treatment with 1,1-carbonydiimidazole and subsequently reacted with a dispersion of amino-functionalised Fe-MIL-101 in DMF at room temperature. PXRD confirmed retention of the MIL-101 structure and ICP-MS revealed 37.3% of the available NH_2-BDC groups were functionalised giving a Pd loading of around 12.8 wt%. Instability of the Fe-MIL-101 particles in PBS buffer necessitated that a thin silica coating be applied to the particles which dramatically lowered the rate of drug release. Silica coated and *cis*-platin-loaded Fe-MIL-101 particles were evaluated to determine their anticancer efficacy against the HT-29 cell line. The MOF drug conjugate showed appreciable cytotoxicity compared with *cis*-platin (IC_{50} of 29 vs 20 μM). Notably this could be enhanced to 21 μM by coating the MOF particles with a cyclic peptide known to target $\alpha_v\beta_3$-integrin, which is over-expressed in many angiogenic tumours. This work further demonstrates the broad utility of PSMet strategies, this time allowing for the incorporation of a metal-based drug

molecule, and points to significant scope for administering metal containing drugs,[97] particularly those that may be prone to degradation in vivo (e.g. NAMI-A).

4. Conclusion and outlook

PSMet has proven to be a versatile and effective strategy for tailoring the properties of MOFs. Here we have outlined the main strategies for PSMet and highlighted some important examples where the technique has been employed to enhance or generate functionality of the host framework. All PSMet approaches display individual merits but some key themes for successful PSMet chemistry can be elucidated. Routes that limit the number of post-synthetic steps give metalated materials that retain the desirable MOF properties of crystallinity and permanent porosity. One step, direct attachment of preformed metal complexes or organometallic precursors, direct linker exchange or the introduction of pore localised metal catalysts by exchange of extra-framework cations typify this observation. Such routes also take advantage of the vast array of existing MOF materials and allow the choice of MOF to be governed by factors related to the application such as chemical stability or pore shape and size. Earlier strategies relied upon careful linker design (to allow PSM) or HSAB theory to generate sites for PSMet impose some limitations on the available MOF structures. However, PSMet addition strategies relying on these approaches provide covalent anchoring of the extraneous metal centre which may offer advantages over pore localised PSMet materials formed by exchange; the metal positioning in the materials with coordinating sites is precise whereas metal complexes added to the pores are free to move. Such positioning can be used to control access, stabilise or otherwise direct the chemistry occurring at a particular post-synthetically modified site.

Recent advances have clearly demonstrated the utility of PSMet, especially with respect to catalysis and improved gas adsorption/separation. Some of the more exciting developments in PSMet chemistry of MOFs point towards future studies aimed at integrating increasingly complex metal species into pore networks. For example, diffusion of metalloproteins or using linker exchange to incorporate functionally complex catalysts are two salient examples. Building on this work, one can envisage that further progress in the area of PSMet may be realized by

using MTV MOF platforms.[98] In such cases complimentary functionalities could be incorporated into a single framework leading to applications such as cascade catalysis.[99]

To fully elaborate the scope of PSMet there are still challenges that need to be addressed. For example, general strategies for improving the efficiency of metalation and establishing protocols for precise structural characterization of the metalated species would lead to insight into applications through greater knowledge of the active entity. It is clear that the progress in PSMet chemistry has tracked with developments in the design and synthesis of MOFs and thus it is expected that this strategy will continue to see rapid growth and lead to novel applications for MOFs.

5. References

1. H. Furukawa, K. E. Cordova, M. O'Keeffe and O. M. Yaghi, *Science*, 2013, **341**, 974.

2. M. Li, D. Li, M. O'Keeffe and O. M. Yaghi, *Chem. Rev.*, 2014, **114**, 1343–1370.

3. C. K. Brozek, M. Dincă, *Chem. Soc. Rev.*, 2014, DOI: 10.1039/C4CS00002A

4. O. M. Yaghi, M. O'Keeffe, N. W. Ockwig, H. K. Chae, M. Eddaoudi and J. Kim, *Nature*, 2003, **423**, 705-714.

5. R. Robson, *Dalton Trans.*, 2008, **38**, 5113-5131.

6. D.-Y. Hong, Y. K. Hwang, C. Serre, G. Férey and J.-S. Chang, *Adv. Funct. Mater.*, 2009, **19**, 1537-1552.

7. J. H. Cavka, S. Jakobsen, U. Olsbye, N. Guillou, C. Lamberti, S. Bordiga and K. P. Lillerud, *J. Am. Chem. Soc.*, 2008, **130**, 13850-13851.

8. C.-D. Wu, A. Hu, L. Zhang and W. Lin, *J. Am. Chem. Soc.*, 2005, **127**, 8940-8941.

9. E. D. Bloch, D. Britt, C. Lee, C. J. Doonan, F. J. Uribe-Romo, H. Furukawa, J. R. Long and O. M. Yaghi, *J. Am. Chem. Soc.*, 2010, **132**, 14382-14384.

10. F. Carson, S. Agrawal, M. Gustafsson, A. Bartoszewicz, F. Moraga, X. Zou and B. Martín-Matute, *Chem. Eur. J.*, 2012, **18**, 15337-15344.

11. T. Jacobs, R. Clowes, A. I. Cooper and M. J. Hardie, *Angew. Chem. Int. Ed.*, 2012, **51**, 5192-5195.

12. D. Feng, W.-C. Chung, Z. Wei, Z.-Y. Gu, H.-L. Jiang, Y.-P. Chen, D. J. Darensbourg and H.-C. Zhou, *J. Am. Chem. Soc*., 2013, **135**, 17105-17110.

13. W. Morris, B. Volosskiy, S. Demir, F. Gándara, P. L. McGrier, H. Furukawa, D. Cascio, J. F. Stoddart and O. M. Yaghi, *Inorg. Chem*., 2012, **51**, 6443-6445.

14. X.-P. Zhou, Z. Xu, M. Zeller, A. D. Hunter, S. S.-Y. Chui, C.-M. Che and J. Lin, *Inorg. Chem.*, 2010, **49**, 7629-7631.

15. X.-P. Zhou, Z. Xu, M. Zeller and A. D. Hunter, *Chem. Commun.*, 2009, 5439-5441.

16. K. L. Mulfort, O. K. Farha, C. L. Stern, A. A. Sarjeant and J. T. Hupp, *J. Am. Chem. Soc.*, 2009, 131, 3866–3868.

17. D. Himsl, D. Wallacher and M. Hartmann, *Angew. Chem. Int. Ed*., 2009, **48**, 4639-4642.

18. Q.-R. Fang, D.-Q. Yuan, J. Sculley, J.-R. Li, Z.-B. Han and H.-C. Zhou, *Inorg. Chem.*, 2010, **49**, 11637-11642.

19. J. He, M. Zha, J. Cui, M. Zeller, A. D. Hunter, S.-M. Yiu, S.-T. Lee and Z. Xu, *J. Am. Chem. Soc.*, 2013, **135**, 7807-7810.

20. K.-K. Yee, N. Reimer, J. Liu, S.-Y. Cheng, S.-M. Yiu, J. Weber, N. Stock and Z. Xu, *J. Am. Chem. Soc*., 2013, **135**, 7795-7798.

21. A. J. Nuñez, L. N. Shear, N. Dahal, I. A. Ibarra, J. W. Yoon, Y. K. Hwang, J.-S. Chang and S. M. Humphrey, *Chem. Commun.*, 2011, **47**, 11855-11857.

22. A. J. Nuñez, M. S. Chang, I. A. Ibarra and S. M. Humphrey, *Inorg. Chem.*, 2014, **53**, 282-288.

23. Z. Wang and S. M. Cohen, *J. Am. Chem. Soc.*, 2007, **129**, 12368-12369.

24. M. J. Ingleson, J. P. Barrio, J.-B. Guilbaud, Y. Z. Khimyak and M. J. Rosseinsky, *Chem. Commun*., 2008, 2680-2682.

25. W. Morris, C. J. Doonan, H. Furukawa, R. Banerjee and O. M. Yaghi, *J. Am. Chem. Soc.*, 2008, **130**, 12626-12627.

26. C. J. Doonan, W. Morris, H. Furukawa and O. M. Yaghi, *J. Am. Chem. Soc.*, 2009, **131**, 9492-9493.

27. K. K. Tanabe and S. M. Cohen, *Angew. Chem. Int. Ed.*, 2009, **48**, 7424-7427.

28. T. Gadzikwa, O. K. Farha, K. L. Mulfort, J. T. Hupp and S. T. Nguyen, *Chem. Commun.*, 2009, 3720-3722.

29. K. M. L. Taylor-Pashow, J. Della Rocca, Z. Xie, S. Tran and W. Lin, *J. Am. Chem. Soc.*, 2009, **131**, 14261-14263.

30. S. Bhattacharjee, D.-A. Yanga and W.-S. Ahn, *Chem. Commun.*, 2011, **47**, 3637-3639.

31. J. Canivet, S. Aguado, Y. Schuurman and D. Farrusseng, *J. Am. Chem. Soc*., 2013, **135**, 4195-4198.

32. K. K. Tanabe, C. A. Allen and S. M. Cohen, *Angew. Chem. Int. Ed.*, 2010, **49**, 9730-9733.

33. T. Yamada and H. Kitagawa, *J. Am. Chem. Soc*., 2009, **131**, 6312-6313.

34. D. Rankine, A. Avellaneda, M. R. Hill, C. J. Doonan and C. J. Sumby, *Chem. Commun.*, 2012, **48**, 10328-10330.

35. H. G. T. Nguyen, M. H. Weston, A. A. Sarjeant, D. M. Gardner, Z. An, R. Carmieli, M. R. Wasielewski, O. K. Farha, J. T. Hupp and S. T. Nguyen, *Cryst. Growth Des.*, 2013, **13**, 3528-3534.

36. A. Vimont, H. Leclerc, F. Maugé, M. Daturi, J,-C. Lavalley, S. Surblé, C. Serre and G. Férey, *J. Phys. Chem.*, 2007, **111**, 383-388.

37. Y. K. Hwang, D.-Y. Hong, J.-S. Chang, S. H. Jhung, Y.-K. Seo, J. Kim, A. Vimont, M. Daturi, C. Serre, and G. Férey, *Angew. Chem. Int. Ed.*, 2008, **47**, 4144-4148.

38. T. Loiseau, C. Serre, C. Huguenard, G. Fink, F. Taulelle, M. Henry, T. Bataille and G. Férey, *Chem. Eur. J.*, 2010, **10**, 1373-1382.

39. M. Meilikhov, K. Yusenko and R. A. Fischer, *J. Am. Chem. Soc.*, 2009, **131**, 9644-9645.

40. H. T. Nguyen, M. H. Weston, O. K. Farha, J. T. Hupp and S. T. Nguyen, *CrystEngComm*, 2012, **14**, 4115-4118.

41. S. Takaishi, E. J. DeMarco, M. J. Pellin, O. K. Farha and J. T. Hupp, *Chem. Sci.*, 2013, **4**, 1509-1513.

42. S. Pullen, H. Fei, A. Orthaber, S. M. Cohen and S. Ott, *J. Am. Chem. Soc.*, 2013, **135**, 16997-17003.

43. M. Kim, J. F. Cahill, H. Fei, K. A. Prather and S. M. Cohen, *J. Am. Chem. Soc.*, 2012, **134**, 18082-18088.

44. S. S. Kaye and J. R. Long, *J. Am. Chem. Soc.*, 2008, **130**, 806-807.

45. S. Chavan, J. G. Vitillo, M. J. Uddin, F. Bonino, C. Lamberti, E. Groppo, K.-P. Lillerud and S. Bordiga, *Chem. Mater.*, 2010, **22**, 4602-4611.

46. K. L. Mulfort and J. T. Hupp, *J. Am. Chem. Soc.*, 2007, **129**, 9604-9605.

47. P. V. Dau, M. Kim and S. M. Cohen, *Chem*. *Sci.*, 2013, **4**, 601–605.

48. C. Wang, J.-L. Wang and W. Lin, *J. Am. Chem. Soc.*, 2012, **134**, 19895-19908.

49. R. S. Crees, M. L. Cole, L. R. Hanton and C. J. Sumby, *Inorg. Chem.*, 2010, **49**, 1712-1719.

50. G.-Q. Kong, X. Xu, C. Zou and C.-D. Wu, *Chem. Commun.*, 2011, **47**, 11005-11007.

51. G.-Q. Kong, S. Ou, C. Zou and C.-D. Wu, *J. Am. Chem. Soc.*, 2012, **134**, 19851-19857.

52. S. Yang, X. Lin, A. J. Blake, G. S. Walker, P. Hubberstey, N. R. Champness and M. Schröder, *Nat. Chem.*, 2009, **1**, 487-492.

53. S. Yang, G. S. B. Martin, J. J. Titman, A. J. Blake, D. R. Allan, N. R. Champness, and M. Schröder, *Inorg. Chem.*, 2011, **50**, 9374-9384.

54. J. An, S. J. Geib and N. L. Rosi, *J. Am. Chem. Soc.*, 2009, **131**, 8376-8377.

55. J. An, C. M. Shade, D. A. Chengelis-Czegan, S. Petoud and N. L. Rosi, *J. Am. Chem. Soc.*, 2011, **133**, 1220-1223.

56. P. Wang, J.-P. Ma , Y.-B. Dong and R.-Q. Huang, *J. Am. Chem. Soc.*, 2007, **129**, 10620-10621.

57. M. Dincă and J. R. Long, *J. Am. Chem. Soc.*, 2007, **129**, 11172-11176.

58. A. M. Shultz, A. A. Sarjeant, O. K. Farha, J. T. Hupp and S. T. Nguyen, *J. Am. Chem. Soc.*, 2011, **133**, 13252-13255.

59. A. M. Shultz, O. K. Farha, D. Adhikari, A. A. Sarjeant, J. T. Hupp and S. T. Nguyen, *Inorg. Chem.*, 2011, **50**, 3174-3176.

60. X.-S. Wang, M. Chrzanowski, L. Wojtas, Y.-S. Chen and S. Ma, *Chem. Eur. J.*, 2013, **19**, 3297–3301.

61. Z. Zhang, L. Zhang, L. Wojtas, P. Nugent, M. Eddaoudi and M. J. Zaworotko, *J. Am. Chem. Soc.*, 2012, **134**, 924-927.

62. F. Nouar, J. Eckert, J. F. Eubank, P. Forster and M. Eddaoudi, *J. Am. Chem. Soc.*, 2009, **131**, 2864-2870.

63. W.-G. Lu, L. Jiang, X.-L. Feng and T.-B. Lu, *Inorg. Chem.*, 2009, **48**, 6997-6999.

64. Z. Zhang, W.-Y. Gao, L. Wojtas, S. Ma, M. Eddaoudi, M. J. Zaworotko, *Angew. Chem. Int. Ed.*, 2012, **51**, 9330-9334.

65. H. Deng, S. Grunder, K. E. Cordova, C. Valente, H. Furukawa, M Hmadeh, F. Gándara, A. C. Whalley, Z. Liu, S. Asahina, H. Kazumori, M. O'Keeffe, O. Terasaki, J. F. Stoddart, O. M. Yaghi, *Science*, 2012, **336**, 1018-1023.

66. C.-Y. Sun, X.-L. Wang, X. Zhang, C. Qin, P. Li, Z.-M. Su, D.-X. Zhu, G.-G. Shan, K.-Z. Shao, H. Wu and J. Li, Nat. Commun., 2013, 4:2717, DOI: 10.1038/ncomms371.

67. J. Yu, Y. Cui1, C. Wu, Y. Yang, Z. Wang, M. O'Keeffe, B. Chen and G. Qian, *Angew. Chem. Int. Ed*., 2012, **51**, 10542-10545.

68. D. T. Genna, A. G. Wong-Foy, A. J. Matzger and M. S. Sanford, *J. Am. Chem. Soc.*, 2013, **135**, 10586–10589.

69. H. Kim, H. Chun, G.-H. Kim, H.-S. Leeb and K. Kim, *Chem. Commun*., 2006, 2759-2761.

70. S. Hermes, F. Schröder, S. Amirjalayer, R. Schmida and R. A. Fischer, *J. Mater. Chem.*, 2006, **16**, 2464-2472.

71. G. Lu, S. Li, Z. Guo, O. K. Farha, B. G. Hauser, X. Qi, Y. Wang, X. Wang, S. Han, X. Liu, J. S. DuChene, H. Zhang, Q. Zhang, X. Chen, J. Ma, S. C. J. Loo, W. D. Wei, Y. Yang, J. T. Hupp and F. Huo, *Nat. Chem.*, 2012, **4**, 310-316 and references therein.

72. G. Férey, C. Mellot-Draznieks, C. Serre, F. Millange, J. Dutour, S. Surblé and I. Margiolaki, Science, 2005, **309**, 2040-2042.

73. N.V. Maksimchuk, M.N. Timofeeva, M.S. Melgunov, A.N. Shmakov, Yu.A. Chesalov, D.N. Dybtsev, V.P. Fedin, O.A. Kholdeeva, *J. Catal*., 2008, **257**, 315-323.

74. N. V. Maksimchuk, K. A. Kovalenko, S. S. Arzumano, Y. A. Chesalov, M. S. Melgunov, A. G. Stepanov, V. P. Fedin and O. A. Kholdeeva, *Inorg. Chem*., 2010, **49**, 2920-2930.

75. V. Lykourinou, Y. Chen, X.-S. Wang, L. Meng, T. Hoang, L.-J. Ming, R. L. Musselman and S. Ma, *J. Am. Chem. Soc.*, 2011, **133**, 10382-10385.

76. H.-L. Jianga and Q. Xu, *Chem. Commun.*, 2011, **47**, 3351-3370.

77. M. Meilikhov, K. Yusenko, D. Esken, S. Turner, G. Van Tendeloo and R. A. Fischer, *Eur. J. Inorg. Chem.*, 2010, 3701–3714.

78. S. Hermes, M.-K. Schröter, R. Schmid, L. Khodeir, M. Muhler, A. Tissler, R. W. Fischer and R. A. Fischer, *Angew. Chem. Int. Ed.*, 2005, **44**, 6237-6241.

79. F. Schröder, D. Esken, M. Cokoja, M. W. E. van den Berg, O. I. Lebedev, G. Van Tendeloo, B. Walaszek, G. Buntkowsky, H.-H. Limbach, B. Chaudret and R. A. Fischer, *J. Am. Chem. Soc.*, 2008, **130**, 6119-6130.

80. M. Müller, X. Zhang, Y. Wang and R. A. Fischer, *Chem. Commun.*, 2009, 119-121.

81. Y. K. Hwang, D.-Y. Hong, J.-S. Chang, S. H. Jhung, Y.-K. Seo, Ji. Kim, A. Vimont, M. Daturi, C. Serre, and G. Férey, *Angew. Chem. Int. Ed.*, 2008, **47**, 4144-4148.

82. T.-H. Park, A. J. Hickman, K. Koh, S. Martin, A. G. Wong-Foy, M. S. Sanford and A. J. Matzger, *J. Am. Chem. Soc.*, 2011, **133**, 20138-20141.

83. B. Nepal and S. Das, *Angew. Chem. Int. Ed.*, 2013, 52, 7224-7227.

84. R. E. Hansen and S. Das, *Energy Environ. Sci.* , 2014, **7**, 317-322.

85. A. Corma and H. Garcia, *Eur. J. Inorg. Chem*., 2004, 1143-1164.

86. B. Li, Y. Zhang, D. Ma, T. Ma, Z. Shi and S. Ma, *J. Am. Chem. Soc.*, 2014, **136**, 1202-1205.

87. L. Ma, J. M. Falkowski, C. Abney and W. Lin, *Nat. Chem.*, 2010, **2**, 838-847.

88. P. V. Dau and S. M Cohen, *Chem. Commun.*, 2013, **49**, 6128-6130.

89. M. Sabo, A. Henschel, H. Fröde, E. Klemmb and S. Kaskel, *J. Mater. Chem.*, 2007, **17**, 3827-3832.

90. S. R. Caskey, A. G. Wong-Foy and A. J. Matzger, *J. Am. Chem. Soc.*, 2008, **130**, 10870-10871.

91. H. Wu, W. Zhou and T. Yildirim, *J. Am. Chem. Soc.*, 2009, **131**, 4995-5000.

92. D. Britt, H. Furukawa, B. Wang, T. G. Glover and O. M. Yaghi, *Proc. Nat. Acad. Sci.*, 2009, **106**, 20637-20640.

93. S. S. Han and W. A. Goddard III, *J. Am. Chem. Soc.*, 2007, **129**, 8422-8423.

94. R. B. Getman, J. H. Miller, K. Wang and R. Q. Snurr, *J. Phys. Chem. C.*, 2011, **115**, 2066-2075.

95. J. Liu, D. M. Strachana and P. K. Thallapally, *Chem. Commun*., 2014, **50**, 466-468.

96. M. Carboni, C. W. Abney, S. Liu and W. Lin, *Chem. Sci.*, 2013, **4**, 2396-2402.

97. T. W. Hambley, *Dalton Trans*., 2007, 4929-4937.

98. H. Deng, C. J. Doonan, H. Furukawa, R. B. Ferreira, J. Towne, C. B. Knobler, B. Wang and O. M. Yaghi, *Science*, 2010, **327**, 846-850.

99. D. E. Fogg and E.N. dos Santos, *Coord. Chem. Rev.*, 2004, **248**, 2365-2379.

Author Biographies

Jack Evans

Jack Evans was born in Adelaide, South Australia. He obtained a BSc(Hons) in Chemistry from the University of Adelaide (UofA) in 2011. Shortly thereafter, he began his PhD at UofA with support from the Commonwealth Scientific and Industrial Research Organisation (CSIRO). This support has allowed him time to visit and work with the research group of Professor David Sholl at the Georgia Institute of Technology. His research areas include porous materials, molecular simulations and environmentally relevant gas separations.

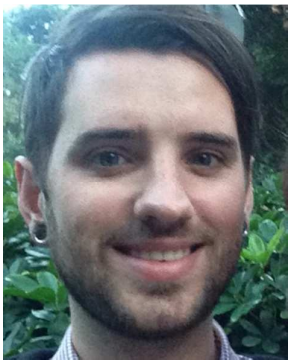

Christopher Sumby

Chris Sumby was born and raised in Christchurch, New Zealand and completed a BSc(Hons) and PhD degrees at the University of Canterbury. He held post-doctoral and fellowship positions at the University of Leeds and the University of Otago before taking up a position at the University of Adelaide in 2007, where he undertakes research into the synthesis and properties of nanomaterials to address energy and environmental challenges. He was an Australian Research Council Future Fellow from 2010 to 2014 and has been awarded various fellowships and awards, including a South Australian Young Tall Poppy (2009) and a Japan Society for the Promotion of Science International Invitational Fellowship (2013-14).

Christian Doonan

Christian Doonan was born in Melbourne, Australia and received undergraduate and PhD degrees from the University of Melbourne. Christian was introduced to MOFs in the laboratory of Prof. Omar Yaghi at UCLA as a post doctoral fellow. Subsequent to this he moved to the University of Adelaide where he is now Associate Professor and Director of the Centre for Advanced Nanomaterials. Christian is currently an Australian Research Council Future Fellow and was selected as an emerging leader as part of the Japan-Australia Emerging Leaders Research Program 2013 and was awarded a JSPS visiting fellowship in 2014. Additionally, he is a frequent visitor to the McLaren Vale and Barossa Valley.

TOC graphic